Eidgenössische Technische Hochschule Zürich
Swiss Federal Institute of Technology Zurich

IMRT Measurement and Control Laboratory

Andreas Isler & Tobias Baltensperger

Modeling of the New Monte Rosa Lodge and Determination of an Optimal Control Signal

Bachelor Thesis

Measurement and Control Laboratory
Swiss Federal Institute of Technology (ETH) Zurich

Supervision

Prof. Dr. Lino Guzzella

December 2008

Preface

This thesis was made possible with support of several members of the IMRT and the project partners of the New Monte Rosa Project.
Special thanks go to Prof. L. Guzzella who supervised the work personally and makes the whole project possible at the IMRT.
From the IMRT team Roland Bucher was a special help for the contact to the other project partners. Daniel Ambühl, Olle Sundström and Christian Dönitz also from IMRT supported the work greatly during the optimization process and Samuel Fux who continues the project at the IMRT was a great support in the final phase of documenting the results.
Further thanks go to the House Automation Team of the University of Applied Science Luzern, especially to Iwan Plüss and Urs-Peter Menti, whose work was a good fundament to base this thesis on.
The engineering team of the Lauber IWISA AG was a big help during the modeling process. A special thank goes to Beat Loosli, who explained several cloudy points about the house automation and helped to find the correct contact person for each house automation component.
And finally special thanks go to our parents and friends who supported us in language concerns and in many other ways.

Contents

Abstract

This thesis is part of the project around the New Monte Rosa Lodge of the Swiss Alpine Club (SAC). The lodge is built almost $2900m$ above sea level and is not connected to any energy or water supply grid. However, it has an extended house automation, consisting of thermal solar collectors and photovoltaic cells, water tanks which store heat, a battery and a combined heat and power plant which can startup if there is an energy shortage. The lodge is constructed by different project partners as a jubilee project for 150 years ETH Zurich. The Measurement and Control Laboratory IMRT is responsible for the development of an advanced model predictive control algorithm which will increase the grade of autarky of the New Monte Rosa Lodge, meaning that the overall fuel consumption is minimized.

First a mathematical model of the new lodge and its house automation is derived. Also booking schedule and weather forecast data are included in the model. In a second step a linear and a dynamic programming algorithm are implemented in order to compute the minimum possible fuel consumption by determining the best control input sequence for all house automation parts.

The model consist of differential and algebraic equations which are derived from fundamental laws of physics and from information supplied by project partners of the New Monte Rosa Lodge. The equations are set up such that they represent the essential dynamics accurately and are easy enough for an optimization algorithm to deal with. Former asks for a lot of states while latter requires the state space to be as small as possible. Both needs are successfully merged into a model with 6 states. The equations are implemented in MATLAB® Simulink® in order to simulate the system over time.

In order to determine the optimal control input sequence the model is split up in an electrical and a thermal part. These two subsystems are optimized separately with a linear respectively a dynamic programming algorithm. The lost interconnection between the two subsystems due to the split is discussed and analyzed. Furthermore, a heuristic controller is developed to which the behavior of the optimized controller can be compared.

The results derived, based on weather and booking schedule data from the year 2006, show the typical behavior of the different control strategies during three different time periods. The advantages of an optimized controller are outlined and discussed.

List of Symbols

Indices

0	Initial
a	Ambient
air	Air
eH_WWTP	Electric Heating into the Room where the WWTP is installed
env	Environment
max	Maximum
min	Minimum
persons	Persons
solar	Thermal Solar Collectors
stoch	Stochastic
sun	Solar Irradiation on Building
warmDrinkingWater	Warm Drinking Water
wasteWater_in	Waste Water Entering the Waste Water Tank
wasteWater_out	Waste Water Exiting the Waste Water Tank
wasteWaterTank_SOC	SOC of the Waste Water Tank
B	Building
eH_HTS	Electric Heating into the HTS
HA	House Automation
HS	Heating System
HTS	High Temperature Storage
HTS_LTS	From the High Temperature Storage to the Low Temperature Storage
HTS2LTS	From the High Temperature Storage to the Low Temperature Storage
LTS	Low Temperature Storage
LTS2HS	From the Low Temperature Storage to the Heating System
PE	Power Electronics
TSC	Thermal Solar Collectors
TSC_HTS	From the Thermal Solar Collectors to the High Temperature Storage

TSC_LTS	From the Thermal Solar Collectors to the Low Temperature Storage
TSC_WDWS	From the Thermal Solar Collectors to the Warm Drinking Water Storage
VS	Ventilation System
WDWS	Warm Drinking Water Storage

Ancronyms and Shortcuts

ctr	Control Signal
CHP	Combined Heat and Power Plant
DP	Dynamic Program / Dynamic Programming
ETH	Eidgenössische Technische Hochschule / Swiss Federal Institute of Technology
HA	House Automation
HS	Heating System
HTS	High Temperature Storage
HVAC	Heating, Ventilating and Air Conditioning
HX	Heat Exchanger
LP	Linear Program / Linear Programming
LTS	Low Temperature Storage
HTS	High Temperature Storage
MPC	Model Predictive Control / Model Predictive Controller
PE	Power Electronics
PID	PID-Controller: A Controller Consisting of a Proportional, an Integrating and a Differentiating Part
PV Cell	Photovoltaic Cell
QP	Quadratic Program / Quadratic Programming
SAC	Swiss Alpine-Club
SOC	State of Charge
TSC	Thermal Solar Collectors
VS	Ventilation System

WDWS	Warm Drinking Water Storage
WWTP	Waste Water Treatment Plant

Symbols

c	Heat Capacity / Constant	$[-]$
ctr	Control Signal	$[-]$
A	Area	$[m^2]$
E	Electric Energy	$[J]$
$\dot{\text{E}}$	Power	$[W]$
goa	Grade of Autarky	$[\%]$
m	Mass	$[kg]$
$\dot{\text{m}}$	Mass Flow	$[\frac{kg}{s}]$
P	Electric Power	$[W]$
T	Temperature	$[K]$
Q	Heat	$[J]$
$\dot{\text{Q}}$	Heat Flow	$[W]$
U	Heat Conduction Coefficient	$[\ \frac{W}{m^2 \cdot K}\ ]$
V	Volume	$[m^3]$
$\dot{\text{V}}$	Volume Flow	$[\frac{m^3}{s}]$
η	Efficiency	$[-]$

Chapter 1

Introduction

1.1 Motivation

This bachelor thesis is part of the project around the New Monte Rosa Lodge of the Swiss Alpine Club (SAC). The lodge is constructed by different project partners as a jubilee project for 150 years of ETH Zurich. All these ETH projects have the same motivation: to make a sustainable contribution to the society. The increasing energy consumption and CO_2 production is a problem we are faced with every day. In the last decades the main objective was to reduce the fuel consumption of transportation. But since a few years the demand for energy saving technologies for buildings is constantly increasing. Indeed, the potential to save energy in facilities is much larger than that for the transportation sector [13].
With regard to the lodge, the most expensive issue related to energy saving aspects are the helicopter transports, which are necessary to bring fuel, food and other supplies. If the lodge had a high energy independency, the number of flights could be reduced substantially. The goal of the New Monte Rosa Lodge project is to

Figure 1.1.0.1: Montage of the New Monte Rosa Lodge.

build a new lodge that reaches a grade of autarky above 90% [1]. This goal shall be reached by an intelligent usage of the locally accumulated solar energy and correctly chosen HVAC components. Intelligent usage means to synchronize the operation of the components with a predictive control system. Today, buildings are rarely handled as integrated systems; normally, each component of a building is controlled separately. These simple controllers are only based on current measurement signals, which can lead to bad decisions. An intelligent controller, like the one to be built in the New Monte Rosa Lodge, is able to take the development of weather conditions and guest reservations into account. Only in this way the ambitious aim of an autarky level above 90% can be reached.

1.2 Initial Position

In the years 2003 to 2005, the faculty of architecture of the ETH Zurich developed the construction of the New Monte Rosa Lodge. Until then, no decisions about the technical components of the lodge were made. This followed in the years 2006 and 2007, when the Lucerne University of Applied Sciences and Arts evaluated fundamental calculations of the thermal and electrical energy need of the lodge. Based on these results, the size of the HVAC components, the photovoltaic cells, the thermal solar collectors etc. was estimated and the final technical equipment was chosen.
In this thesis an optimal allocation of the available energy is computed.

1.3 Tasks & Goals

Actually two tasks are to be solved: The first task is to create a mathematical model of the lodge. This means, that in a first step all components of the building are identified and quantified, which are able to store energy or mass, including the building itself. The second step is to map the interconnections between these storages. In a third step, these relations are represented in a mathematical way such that they can be used for an optimization problem.
The second task is to find an optimal control signal for every adjustable component in the lodge. This control signal shall be optimal in the sense that it minimizes the overall fuel consumption and thus maximizes the grade of autarky. Of course various constraints have to be fulfilled, such as comfortable climate inside the building. The goal is to create a benchmark; the performance of every controller which will be built in the future can be checked against this benchmark.

1.4 Structure of the Thesis

Firstly, some fundamental theory is discussed in Chapter 2. The basic concepts of linear programming and dynamic programming are derived. Secondly, the New Monte Rosa Lodge and its house automation is described in Chapter 3, followed by the description of the modeling process in Chapter 4. Chapter 5 covers the implementation of the optimization algorithms in MATLAB®. The computed results are discussed in Chapter 6.

[1] excluding energy spent on cooking

Chapter 2

Theoretical Foundations

Mathematical models and methods used in the present work are discussed in this chapter. In Section 2.1, the reader is introduced to a systematic approach of transforming physical phenomena into mathematical models and equations. In Section 2.2 some mathematical definitions are given, which are used in Sections 2.3 and 2.4 where the linear programming (LP) and the dynamic programming (DP) are introduced and their theoretical background is described. To give the reader an understanding of their application area their advantages and drawbacks are discussed. An brief introduction to model predictive control (MPC) in Section 2.5 closes this chapter.

2.1 Modeling

The background of the following equations is found in [5].

2.1.1 Basic Approach

First of all one can distinguish two main classes of objects in a physical system:

- "Reservoirs", which typically store mass, energy, charge or information;
- "Flows", i. e., any interaction between reservoirs or a reservoir and the environment.

Reservoirs cause a dynamic effect in a system and have a level variable associated. A reservoir with a large time constant is referred to as a *slow* dynamic, one with a small time constant as a *fast* dynamic. It depends on the problem setting, which dynamics are the interesting ones. If the reaction time of a sensor is asked for some reason, the *relevant dynamics* have time constants in the order of seconds to milliseconds. But if the temperature of a room is of interest, the dynamics with time constants of a second are not at all interesting, all the more the ones with time constants of minutes or even hours.
A typical approach to model a system is the following:

1. Define the boundaries of the system as well as the inputs and outputs;
2. Identify all relevant dynamic elements (in other words, reservoirs) of the system and the corresponding level variable;

3. Formulate the differential equations for all relevant dynamics in the following form:
$$\frac{d}{dt}(\text{reservoir content}) = \sum \text{inflows} - \sum \text{outflows}\,; \tag{2.1}$$
4. Formulate the algebraic relations which describe the flows between the reservoirs and eliminate implicit algebraic loops if possible;
5. Identify the unknown system parameters with some experiments and verify them with independent experiments.

2.1.2 Useful Equations

In Table 2.1.2.1 the most important equations, which were used later to model the lodge, are given in their standard form.

Enthalpy flow	$\dot{H} = c_p \dot{m}\ \mathrm{T}$
Energy conservation	$\frac{d}{dt}E(t) = \dot{Q}_{in} - \dot{Q}_{out}$
Mass conservation	$\frac{d}{dt}m(t) = \dot{m}_{in} - \dot{m}_{out}$

Table 2.1.2.1: Some useful equations

2.2 Mathematical Definitions

Some basic mathematical definitions are given in this section. They provide a basis for Sections 2.3 and 2.4 where the linear programming (LP) and the dynamic programming (DP) are introduced and their theoretical background is described. The notation is based on [2].

Subspaces

$S \subseteq \mathbb{R}^n$ is a *subspace* if

$$x, y \in S, \quad \lambda, \mu \in \mathbb{R} \quad \rightarrow \lambda x + \mu y \in S\,. \tag{2.2}$$

In a three-dimensional space $\mathbb{R}^3$ S is a plane through $0, x, y \subseteq S$.
A subspace can be represented by a matrix in different ways:

$$\begin{aligned} \text{range}(A) &= \{Aw | w \in \mathbb{R}^q\} \\ &= \{w_1 a_1 + \ldots + w_q a_q | w_i \in \mathbb{R}\} \\ &= \text{span}(a_1, a_2, \ldots, a_q)\,, \end{aligned} \tag{2.3}$$

where $A = [a_1, a_2, \ldots, a_q]$.

Affine Sets

$S \subseteq \mathbb{R}^n$ is *affine* if

$$x, y \in S, \quad \lambda, \mu \in \mathbb{R}, \quad \lambda + \mu = 1 \quad \Rightarrow \lambda x + \mu y \in S\,. \tag{2.4}$$

In a three-dimensional space $\mathbb{R}^3$ S is a plane through $x, y \subseteq S$, i. e., a shifted subspace, which no longer goes through the origin.
It can be represented by linear equalities:

$$S \quad = \quad \{x | Ax = b\}\,. \tag{2.5}$$

Convex Sets

$S \subseteq \mathbb{R}^n$ is a *convex set* if

$$x, y \in S, \quad \lambda, \mu \in \mathbb{R}_+, \quad \lambda + \mu = 1 \quad \Rightarrow \lambda x + \mu y \in S\,. \tag{2.6}$$

A convex set has the property, that every point z between two arbitrary points of the set $x, y \in S$ is also part of the set:

$$x, y \in S, \quad h \in [0,1] \Rightarrow z = x + h(y - x) \in S\,. \tag{2.7}$$

Hyperplanes and Halfspaces

A *hyperplane* is defined as follows:

$$\{x | a^T x = b\} (a \neq 0)\,, \tag{2.8}$$

where $x, a \in \mathbb{R}^n, \quad b \in \mathbb{R}$.
A hyperplane is affine and separates a space into two parts.
It is a subspace if $b = 0$.

A *halfspace* is defined as

$$\{x | a^T x \leq b\} (a \neq 0)\,, \tag{2.9}$$

where $x, a \in \mathbb{R}^n, \quad b \in \mathbb{R}$.
A halfspaces is convex.

Intersections

The *intersection* of affine and/or convex subspaces is again an affine or convex subspace.
An important example is the *polyhedron*, which is an intersection of a finite number of halfspaces:

$$\begin{array}{rcl} \mathcal{P} & = & \{x | a_i^T x \leq b_i, \quad i = 1, \ldots, k\} \\ & = & \{x | Ax \preceq b\} \quad (\preceq \text{ means componentwise})\,, \end{array} \tag{2.10}$$

where $x, a_i \in \mathbb{R}^n, \quad A = [a_1, a_2, \ldots, a_k]^T \in \mathbb{R}^{k \times n}, \quad b = [b_1, b_2, \ldots, b_k]^T \in \mathbb{R}^k$.
A closed convex set S is always a polyhedron, i. e., an intersection of halfspaces.

Formulation of an Optimization Problem

$$\begin{array}{ll} \text{minimize} & f_0(x) \\ \text{subject to} & f_i(x) \leq 0, i = 1, \ldots, m \\ & h_i(x) = 0, i = 1, \ldots, p\,, \end{array} \tag{2.11}$$

where $f_i, h_i : \mathbb{R}^n \to \mathbb{R}, \quad x \in \mathbb{R}^n$.

- x is the optimization variable,
  $f_0(x)$ is the objective or cost function,
  $f_i(x) \leq 0$ are the inequality constraints,
  $h_i(x) = 0$ are the equality constraints;
- x is *feasible* if it satisfies the constraints;
- The *feasible set* C is the set of all feasible points;
- The problem is *feasible* if there are feasible points $x \in C$;

- The problem is *unconstrained* if $m = p = 0$;
- If the problem is feasible, at least one point x exists in the set C and its value $f_0(x)$ is the infimum of the values of the objective function within the set $C : f^\star = \inf_{x \in C} f_0(x)$;
- The optimal point is: $x^\star \in C : f_0(x^\star) = f^\star$
  Generally more than one point x minimizes $f_0(x)$, i. e., the solution is a set: $X_{opt} = \{x \in C | f_0(x) = f^\star\}$.

Local and Global Minimum

The local minimum of an arbitrary continuous function is defined as follows:
A point $x \in C$ is the *local minimum* if it satisfies

$$y \in C, ||y - x|| \leq R \Rightarrow f_0(y) \geq f_0(x) \tag{2.12}$$

for some $R > 0$.
x is *globally minimal*, if

$$y \in C \Rightarrow f_0(y) \geq f_0(x) \tag{2.13}$$

is valid.

Convex Functions

A function $f : \mathbb{R}^n \rightarrow \mathbb{R}$ is *convex* if **dom** f is convex for all $x, y \in$ **dom** f, $\theta \in [0, 1]$:

$$f(\theta x + (1 - \theta)y) \leq \theta f(x) + (1 - \theta) f(y)\,. \tag{2.14}$$

f is concave if $-f$ is convex.
An interesting property of a convex function is that it has only one minimum. Therefore the local minimum is also the global one.

2.3 Dynamic Programming

In this section a short introduction to the wide field of dynamic programming is given. The explanations are focused on the theory which is needed to follow the optimization described in Section 5.3 and make no claim to be a complete mathematical description of the problem. This section is based on the introduction to dynamic programming in [6].

2.3.1 Introduction

Dynamic programming is useful to determine the global optimum of an optimization problem. This optimization is generally not limited to any complexity but the problem can easily exceed available calculation resources. There exist two groups of problems in dynamic programming; the stochastic and the deterministic. To which group a problem belongs is determined by the knowledge about the external influences, in control systems known as disturbances. For a deterministic problem all disturbances are assumed to be known in advance. For a stochastic problem the disturbances are only known with a certain variance. This text concentrates on the group of deterministic problems.

2.3.2 Optimal Control Problem stated for a Time-Invariant Discrete-Time System

The time-invariant, discrete-time system examined here is defined as

$$x_{k+1} = f_k\left(x_k, u_k, w_k\right) . \tag{2.15}$$

x_k	Dynamic states, $x_k \in \mathbb{X} \subseteq \mathbb{R}^n$
u_k	Control inputs, $u_k \in \mathbb{U} \subseteq \mathbb{R}^m$
w_k	Known disturbances $\forall t$, $w_k \in \mathbb{W} \subseteq \mathbb{R}^d$
k	$0, 1, 2, \ldots, N-1$
N	Length of the optimization horizon

The aim of an optimal control problem is to find a control input, which minimizes the cost function

$$J_\pi\left(x_0\right) = g_N\left(x_N\right) + \sum_{k=0}^{N-1} g_k\left(x_k, \mu_k\left(x_k\right), w_k\right) . \tag{2.16}$$

J_π	Total cost for x_0 and π
π	Sequence of control inputs, $\{\mu_0, \mu_1, \ldots, \mu_{N-1}\}$
x_0	Initial condition
g_N	Final cost / final state weight
g_k	Cost for step k
μ	Control inputs

Reformulated in one equation. It is to find the optimal control sequence π^0 which minimizes the cost J_π.

$$J^0\left(x_0\right) = \min_\pi J_\pi\left(x_0\right) \tag{2.17}$$

2.3.3 The Principle of Optimality

The basic requirement behind the dynamic programming is the principle of optimality. For this it is assumed that $\pi^o = \left\{\mu_0^o, \mu_1^o, \ldots, \mu_{N-1}^o\right\}$ is the optimal control sequence, which minimizes 2.16. At time i (arbitrary for $i \in [0, N-1]$) this optimal trajectory reaches the point x_i.
Looking at the same optimization problem with the initial condition x_i and the cost-to-go

$$J(x_i) = g_N\left(x_N\right) + \sum_{k=i}^{N-1} g_k\left(x_k, \mu_k\left(x_k\right), w_k\right) , \tag{2.18}$$

the cost from step i to the final step N, shows that the corresponding elements of the optimal control sequence $\pi^o = \left\{\mu_i^o, \mu_{i+1}^o, \ldots, \mu_{N-1}^o\right\}$ are still the same optimal solution. This fact is illustrated in Figure 2.3.3.1.

2.3.4 Algorithm

Applying the principle of optimality the following algorithm is obtained, which is applied backwards in time from $N-1$ to 0:

1. Calculation of the final cost

$$J_N\left(x_N\right) = g_N\left(x_N\right) \tag{2.19}$$

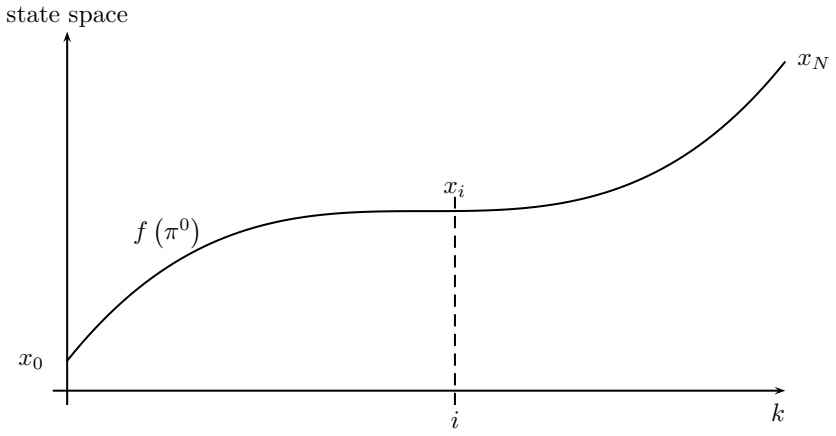

Figure 2.3.3.1: Principle of Optimality: The optimal trajectory for the initial conditions x_0 and x_i is identical from step i to step N.

2. Minimization of the cost-to-go for all steps from $N-1$ to 0

$$J_k\left(x_k\right) = \min_{u_k \in U_k(x_k)} \left\{ g_k\left(x_k, u_k, w_k\right) + J_{k+1}\left(f_k\left(x_k, u_k, w_k\right)\right) \right\} \tag{2.20}$$

The state space system 2.15 is not only discrete in time but also operates with discretized values in valuation space. J_{k+1} is determined for every point of the discretization grid. This is why it has to be interpolated for x_{k+1}, which is related to x_k by the state space equation 2.15, to build the sum in the second algorithm step. This interpolation respectively the discretization of the values has a strong influence on the result and the computing time of the problem. Other influences on the computing time are the number of time steps, states and control inputs. The number of operations to solve a problem is of the following order.

$$\mathcal{O}\left(N \cdot p^n \cdot q^m\right) \tag{2.21}$$

N	Number of time steps
p	Number of possible state values (value discretization)
n	Number of states
q	Number of possible control input values (value discretization)
m	Number of control inputs

This is why this optimization is only applicable to low order systems. If it is not possible to reduce the number of states and inputs further, the discretization precision can be reduced. The weakest influence on the complexity has the number of time steps.

2.4 Linear Programming

The following section on linear programming (LP) is based on [2].
The LP is a subclass of the convex optimization problem.

2.4.1 Convex Optimization Problem

Equations 2.2 - 2.14 allow for defining the optimization problem stated in 2.11 more specific. The standard form of a *convex optimization problem* is as follows:

$$\begin{array}{ll} \text{minimize} & f_0(x) \\ \text{subject to} & f_i(x) \leq 0, \quad i = 1, \ldots, m \\ & a_j^T \cdot x = b_j, \quad j = 1, \ldots, p\,, \end{array} \tag{2.22}$$

where $x \in \mathbb{R}^n, \quad A_{eq} = [a_1, a_2, \ldots, a_p]^T \in \mathbb{R}^{p \times n}, \quad b_{eq} = [b_1, b_2, \ldots, b_p]^T \in \mathbb{R}^p\,,$

- $f_0, f_1, \ldots, f_m : \mathbb{R}^n \to \mathbb{R}$ convex
- all p equality constraints are affine
- the feasible set is convex.

The core of the convex optimization problem is its convex objective function. This type of function has the important property that the local minimum is also the global one. When a convex optimization problem is solved numerically, the global minimum is found very fast. Because of this it is very beneficial to describe the real problem by a convex optimization problem.

2.4.2 Linear Programming

Linear programming (LP) is one application of the convex optimization problem. If all f_i are affine, i. e., $f_i = a_{i,ineq} \cdot x - b_{i,ineq}$, the problem is called a *linear program*:

$$\begin{array}{ll} \text{minimize} & c^T x \\ \text{subject to} & a_{i,ineq}^T \cdot x \leq b_{i,ineq}, \quad i = 1, \ldots, m \\ & a_{j,eq}^T \cdot x = b_{j,eq}, \quad j = 1, \ldots, p\,, \end{array} \tag{2.23}$$

where $x, c, a_{i,ineq}, a_{j,eq} \in \mathbb{R}^n, \quad b_{i,ineq} \in \mathbb{R}^m, \quad b_{i,eq} \in \mathbb{R}^p\ ,$

- m affine inequality constraints; if these m halfspaces intersect, they form a polyhedron
- p affine equality constraints
- the feasible set is convex.

A related problem setup is the *quadratic program* (QP). It differs in the objective function, which is no longer affine, but quadratic.

2.4.3 Optimal Control Problem

In Section 2.3.2 the Optimal Control Problem is stated in a general way for time-invariant discrete-time systems. Assume in addition, that a given system has linear dynamics and affine constraints on the state x and the input u. The Optimal Control Problem can then be written in the following form:

$$J^0(x_0) = \min_{\pi} \quad \sum_{k=0}^{N-1} ||Qx_k||_p + ||Ru_k||_p \tag{2.24}$$

$$\begin{array}{ll} \text{subject to} & x_{k+1} = Ax_k + Bu_k, \quad k \geq 0 \\ & x_k \in \mathbb{X} \subseteq \mathbb{R}^n \\ & u_k \in \mathbb{U} \subseteq \mathbb{R}^m\,, \end{array}$$

where

x_k	State vector x at time k
u_k	Input vector u at time k
p	Typically $p \in \{1, 2, \infty\}$
$\mathbb{X}, \mathbb{U}$	Polyhedral sets
Q, R	Constant matrices of appropriate dimensions
π	Sequence of control signals, $\{\mu_0, \mu_1, \ldots, \mu_{N-1}\}$.

If $p \in \{1, \infty\}$, the problem can be written as a LP; if $p = 2$, the problem can be transformed into a QP.

2.4.4 Transformation of the Optimal Control Problem into a Linear Program

If $p = 1$ is chosen in Equation 2.24, the objective function turns out to be the sum of the next $N - 1$ absolute weighted state and input values. This problem can be transformed into a LP by introducing *decision vectors* Z_x and Z_u, which limit $\mathcal{Q}X$ and $\mathcal{R}U$ from below and from above:

$$\begin{array}{rcl} -Z_x & \leq & \mathcal{Q}X \quad \leq Z_x \\ -Z_u & \leq & \mathcal{R}U \quad \leq Z_u\,, \end{array} \tag{2.25}$$

where

$$\begin{array}{rcll} X & = & [x_0^T & x_1^T \quad \ldots \quad x_{N-1}^T]^T \\ U & = & [u_0^T & u_1^T \quad \ldots \quad u_{N-1}^T]^T \\ \mathcal{Q} & = & \multicolumn{2}{l}{\mathrm{diag}[Q_0, Q_1, \ldots, Q_{N-1}], \quad Q_i \in \mathbb{R}^{n \times n}} \\ \mathcal{R} & = & \multicolumn{2}{l}{\mathrm{diag}[R_0, R_1, \ldots, R_{N-1}], \quad R_i \in \mathbb{R}^{m \times m}\,.} \end{array}$$

The problem can now be written as a LP:

$$\min_{X,U,Z_x,Z_u} \quad \mathbf{1}^T Z_x + \mathbf{1}^T Z_u \tag{2.26}$$

$$\begin{array}{ll} \text{subject to} & \epsilon_u U \leq F_u \\ & \epsilon_x X \leq F_x \\ & -Z_x \leq \mathcal{Q}X \leq Z_x \\ & -Z_u \leq \mathcal{R}U \leq Z_u \\ & [I - \overline{\mathcal{A}}, -\overline{\mathcal{B}}] \cdot [X^T U^T]^T = \mathcal{H} \cdot x_0\,, \end{array}$$

where

$$\begin{array}{rcl} \mathbf{1} & = & [1 \quad 1 \quad \ldots \quad 1]^T \\ \epsilon_u, F_u & & \text{Matrices containing the inequality constraints on u} \\ \epsilon_x, F_x & & \text{Matrices containing the inequality constraints on x} \end{array}$$

$$\overline{\mathcal{A}} = \begin{bmatrix} 0 & 0 & 0 & \ldots & 0 \\ A & 0 & 0 & \ldots & 0 \\ 0 & A & 0 & \ldots & 0 \\ \vdots & \ddots & \ddots & \ddots & \vdots \\ 0 & \ldots & 0 & A & 0 \end{bmatrix}$$

$$\overline{\mathcal{B}} = \begin{bmatrix} 0 & 0 & 0 & \dots & 0 \\ B & 0 & 0 & \dots & 0 \\ 0 & B & 0 & \dots & 0 \\ \vdots & \ddots & \ddots & \ddots & \vdots \\ 0 & \dots & 0 & B & 0 \end{bmatrix}$$

A, B System matrices

$$\mathcal{H} = \begin{bmatrix} I \\ 0 \\ 0 \\ \vdots \\ 0 \end{bmatrix}$$

x_0 Initial condition on the state .

Simplification for x, u $\geq$ 0

If all states x und all inputs u are constrained to be greater or equal to zero, the LP can be written in a simplified way. This is due to the fact, that the 1-norm reduces to a sum and therefore no decision vectors have to be introduced. The LP can be written as

$$\min_{X,U} \quad q^T X + r^T U \tag{2.27}$$

$$\begin{aligned} \text{subject to} \quad & \epsilon_u U \leq F_u \\ & \epsilon_x X \leq F_x \\ & [I - \overline{\mathcal{A}}, -\overline{\mathcal{B}}] \cdot [X^T U^T]^T = \mathcal{H} \cdot x_0 \,, \end{aligned}$$

where the dimensions remain unchanged, except for the weighting matrices $\mathcal{Q}$ and $\mathcal{R}$, which reduce to vectors:

$$\begin{aligned} q &= [q_0^T, q_1^T, \dots, q_{N-1}^T]^T, \quad q_i \in \mathbb{R}^n \\ r &= [r_0^T, r_1^T, \dots, r_{N-1}^T]^T, \quad r_i \in \mathbb{R}^m \,. \end{aligned}$$

Due to this simplification the size of the inequality matrix reduces dramatically.

2.4.5 Solving a Linear Program with MATLAB®

A linear program of the form

$$\begin{aligned} &\text{minimize} && c^T z \\ &\text{subject to} && A_{ineq} \cdot z \leq B_{ineq} \\ & && A_{eq} \cdot z = B_{eq} \end{aligned} \tag{2.28}$$

can be solved in MATLAB® with the following command:

$$z = \text{linprog}(f, A_{ineq}, B_{ineq}, A_{eq}, B_{eq}) \,. \tag{2.29}$$

The five input matrices and vectors contain all necessary information, such as the system equations, the hard and soft constraints and which variable is to be minimized.

2.5 Advantages and Drawbacks of the LP and DP

Both approaches, LP and DP, have their advantages and drawbacks.
A linear program can be solved in very short computing time for thousands of state variables. A large number of states is a prerequisite if a physical problem shall be described sufficiently accurate. However, the physics must be describable in affine equations exclusively, so that these equations can be converted into LP standard form.
A dynamic program takes much longer to be solved, even for just two or three state variables. A program must be computed, which finds the minimum of a non-convex function. As such functions generally have more than one local minimum computing time increases accordingly. Furthermore, the physical problem must be discretized not only in time, but also in magnitude. This explains why the computing time grows exponentially with the number of states. The main advantage is, that the problem can be described with arbitrary complex functions, which gives the freedom to model the physical reality very accurately.

2.6 Outlook: Model Predictive Control

This thesis is a preliminary study for the controller design process. It provides the basis for a model predictive controller (MPC). This chapter briefly describes the concept of a MPC.
The basic idea of this controller concept is to look ahead in time by estimating future disturbances. In contrast to traditional feedback control (e. g., PID control) which always reacts after an event, the MPC can act in advance. This allows the controller to take into account saturation of actuators and other constraints.
The basic algorithm of a MPC can be summarized as follows. Based on a measurement at time step k a MPC determines the optimal trajectory to reach a reference value within the horizon of length N. The particular cost function for the considered problem (i. e., a LP or a DP) is minimized to reach this optimum. The cost function also contains the discrete model of the system and is evaluated for the time span of the horizon. The initial value is the measurement at time step k. The first element of the resulting control sequence is applied to the real system at time step $k + 1$. The whole optimization process restarts with a measurement at time step $k + 1$ to determine the signal applied at time step $k + 2$. Since the model cannot represent the reality perfectly and the optimal solution at one time step does no longer hold for the next one, only the first element of the control sequence is applied (see also Figure 2.6.0.1).
Obviously, the time to solve the optimization must be smaller than the duration of one time step. This is why today MPC is only applied to reasonably simple models or to slow processes. An other factor is the length of the horizon which has a strong influence on the result. Would the horizon be equal to the entire simulation time and the system behavior as well as the environmental influences exactly be known, the MPC would be *ideal*. An ideal MPC calculates a performance bound for the system and the given components that can no be surpassed. Arbitrary control strategies can be compared with this bound and their potential can be determined. For instance it is possible to determine, in which situations a conventional control strategy almost reaches the optimum, and in which situations it is reasonable to implement a MPC to improve the system behavior.

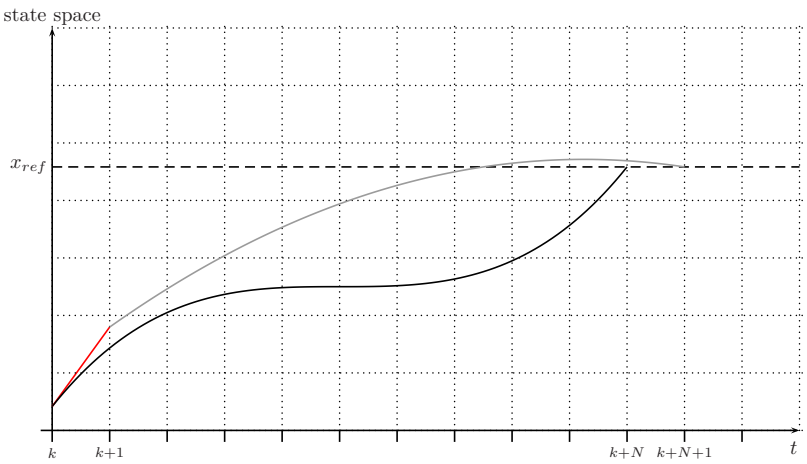

Figure 2.6.0.1: Visualization of the MPC algorithm.
black: optimal trajectory starting from the measurement at k
red: real trajectory
gray: optimal trajectory starting from the measurement at $k+1$

Chapter 3

System Description

3.1 Geography and Climate

The New Monte Rosa Lodge is situated near the Gornergrat and the Duforspitze, between the Gorner Glacier and the Grenz Glacier. It is $2883m$ above sea level. The mean ambient temperature during the time the lodge is maintained (March to September) is $0°C$. In the winter period the ambient temperature decreases to an average of $-5.5°C$ with peaks below $-20°C$. The wind speed is moderate. The peak velocity in the year 2006 is $20m/s$, the mean velocity around $6m/s$ [21].

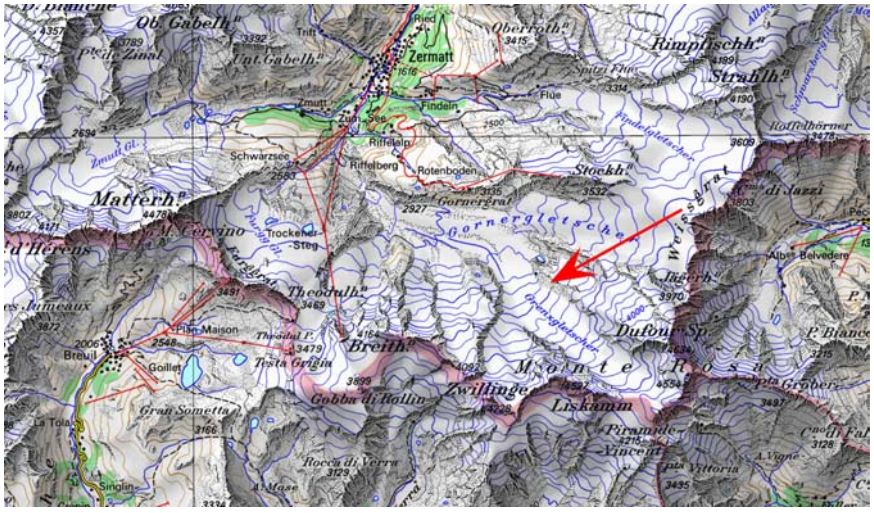

Figure 3.1.0.1: Site of the New Monte Rosa Lodge.
⟨Reproduced with authorization by swisstopo (BA081751)⟩

3.2 Purpose of the Lodge

The New Monte Rosa Lodge is an accommodation for alpinists. It gives them the possibility to stay overnight or just to have a warm meal at noon, before they continue their trip.
The lodge is not connected to the valley by road, it can only be reached by foot by crossing the glaciers. All food and fuel transports are done by helicopter. The lodge is maintained by a caretaker and an assistance team of about five persons.

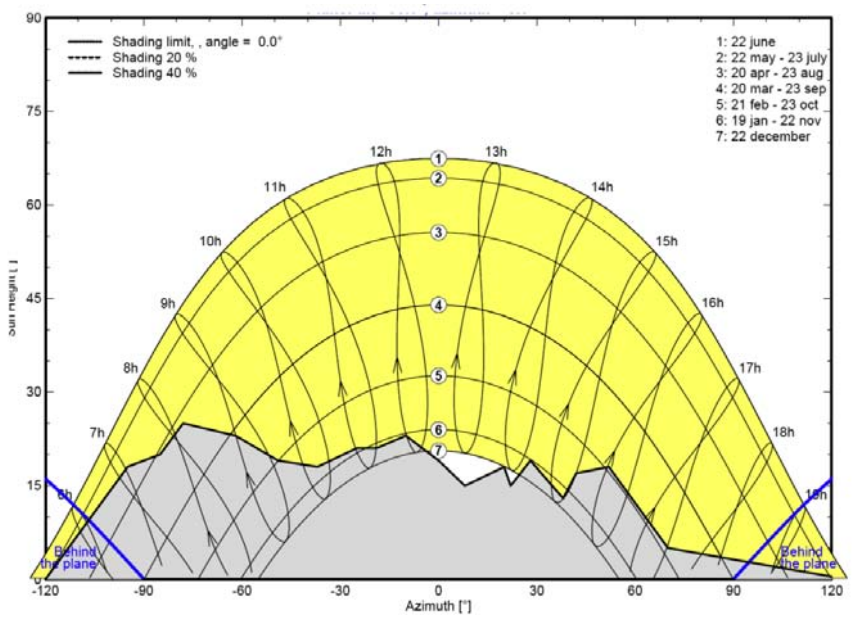

Figure 3.1.0.2: Sun progression at the location of the New Monte Rosa Lodge [16]; in summer the sun exposure of the lodge is 13 hours a day. Notice that solar energy can be obtained only for 2 hours during the shortest winter days.

Their job is to cook meals for the guests, clean the building, make the laundry and manage the administrative tasks, altogether like in a hostel. The traveling alpinists are requested to book their stay in advance, so that the caretaker can plan the amount of food and beds to be ready.

3.3 Structure of the Lodge

The lodge has four floors and two basement levels. The ground floor consists of a kitchen and a restaurant, which is also used as a lounge. On the first, second and third floor are the bedrooms and washrooms. The maintenance team has its own department on the first floor with integrated bathroom and shower. On the first basement level the house automation (HA), the repositories of food, fuel and fresh water and also a drying room for the alpinists' skis and shoes are located. On the second basement level there is a small apartment with a few beds and a kitchenette. This room is not tended to and is opened for guests only in winter, when the rest of the lodge is closed. Furthermore the waste water treatment plant (WWTP) is situated there. The whole building can accommodate a maximum of 120 persons. This is the case at about five weekends per year. On weekdays normally $30 - 40$ people book a bed, on normal weekends up to 60 people. During winter time, when the lodge is not tended to, less then 5 visitors are present most of the time [21].

3.4 Features of the Lodge and the House Automation Components

The entire lodge is very well isolated to minimize energy losses through the hull. There are not a lot of windows, and they can only be opened by the caretaker and his

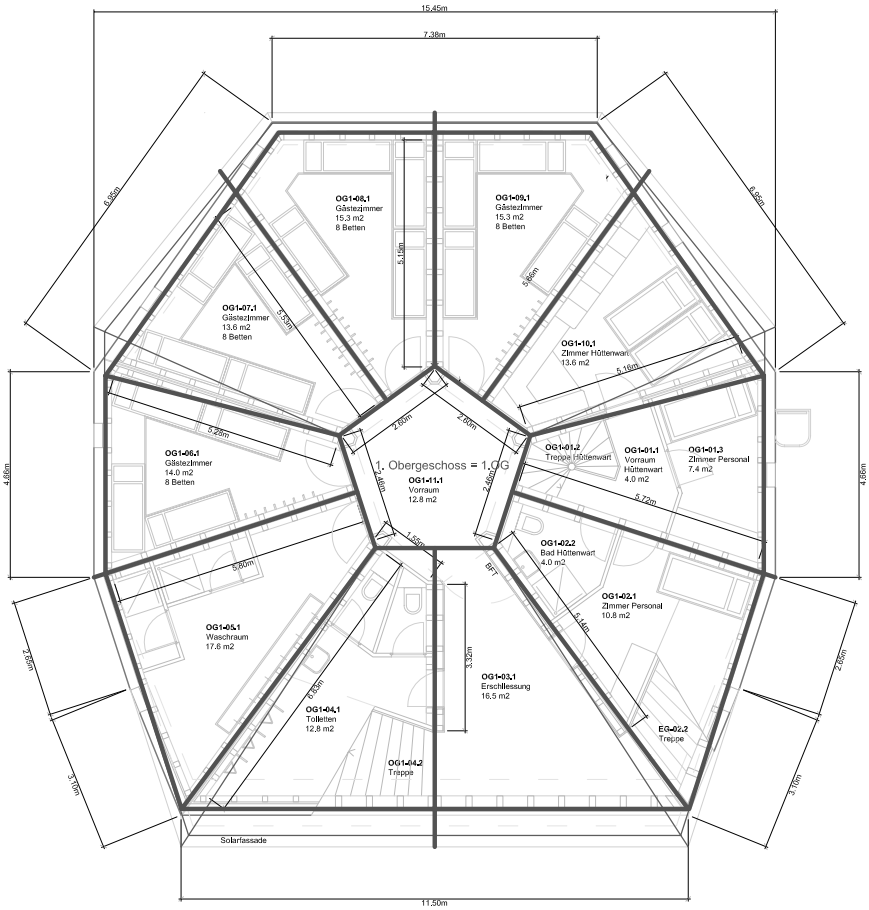

Figure 3.3.0.3: Plan of the first floor [1]; additional plans can be found on the appended CD.

team. The heating system of the building is combined with the ventilation system. Warm air is blown into the building in the restaurant area. Through the stairways the fresh air is transported up to the first, second and third level. Furthermore, the stairway has a window bank, so the sun can heat up the air additionally. The used air is sucked out in each bedroom and shower room. The remaining heat in the air is recuperated.

Figure 3.4.0.4: The stairways of the lodge with a panorama view. Source: [20].

The house automation consists of a warm drinking water tank, two tanks containing heating water, PV cells, thermal solar collectors, a battery, a waste water treatment plant, a combined heat and power supply, a ventilation and heating system, fresh water tanks and a weather station [11] [12] [10].

Thermal Energy Storage

The tank with hot drinkable water has a volume of $270l$. It is embedded in a outer tank with a volume of $1180l$, filled with a 34% glycol-water mixture, referred as heating water. Pure water would freeze and evaporate in the application area. When hot water is consumed by the guests, cold fresh water at $5°C$ from the fresh water supply flows into the hot water tank. The entire tank is called warm drinking water tank (WDWS) [3].
Two additional heating water tanks are installed with a combined capacity of $4400l$. This volume is only separated into two parts because the largest commercial tanks have a volume of $2200l$ [9]. The tanks are connected once in the upper half and once in the lower half and heating water circulates all the time [10]. These two tanks provide energy to heat the building. There is also a controllable connection to the WDWS [10].

PV Cells and Thermal Solar Collectors

The PV cells are installed on the southern side of the building. Its peak power generation is $13.5kW$ [21]. It covers almost the entire electric power demand of the

lodge. Near the building on the ground the thermal solar collectors are installed. They generate a peak power of $58kW$ [21]. The heated 44% glycol-water mixture is transported in an isolated heatable tube into the building. First of all it flows to the WDWS, afterwards to the upper part of the heating tanks, then to the lower part. The controller decides, if the mixture is lead through the heat exchangers in the tanks, or if it just passes the tank because it is colder than the mixture in the tank [10].

Electric Energy Storage

The lead-acid battery is able to store $288kWh$ electric energy [18]. However, the battery should not be discharged under 50% for technological reasons [4]. The battery buffers the electric energy usage and production and is connected by power electronics to the $230V$ isolated network of the lodge [18].

Waste Water Treatment Plant

The waste water treatment plant (WWTP) is situated on the second basement level. Due to this installation it is possible to save a lot of fresh water, because grey water is used to flush the toilets. Furthermore, one can avoid the expensive transport of the waste water down to the valley. Only the highly compressed clearing sludge must be flown down. However, the internal biological system must be held in balance, that is why this installation is the biggest energy consumer. In standby mode it consumes about $700W$, during the cleaning process more than $2kW$ [15].

Combined Heat and Power Plant

The combined heat and power plant(CHP) is a highly efficient electric power generator. The plant is cooled with heating water. Thus over 85% of the energy out of the fuel is used. A part of the remaining 15% are losses into the building. Only a very small percentage is lost through the exhaust.

Ventilation and Heating System

The ventilation- and heating system consist of the following parts [10]:

- A pre-heater, where fresh air from the environment is heated up with heating water to a temperature of about $-7°C$. This component is only active in winter.
- A heat exchanger, in which the incoming air is heated to at least $8°C$ with the energy recuperated from the outgoing air.
- A supplementary heater heats the air up to the desired temperature with heating water.

The outgoing air only passes the heat exchanger and is then blown out to the environment.

Fresh Water Supply Reservoir

$400m$ from the building three fresh water tanks are situated. The tanks together store $140m^3$ melt water, which accrues during summer. This amount is enough to supply the lodge during the whole year [16].

Weather Station

Next to the lodge a weather station is installed, which collects data so that a local weather forecast will be possible in future. Up to then the weather data is interpolated from three weather stations near-by.

3.5 Constraints

Various constraints resulting from the lodge's purpose or requirements of the Swiss Alpine Club [17] are listed here:

- The lodge is maintained in the months March to May and July to September
- 6500 persons per year eat a warm meal in the evening and stay over night
- 2000 persons per year have a warm meal at noon
- On 5 weekends per year the lodge is booked up. 120 persons stay over night and 40 guests eat warm at noon
- Minimal temperature in the guestrooms is $5°C$, target value is $20°C$ [16].
- Minimal temperature in the restaurant and in the kitchen is $15°C$, the target value is $20°C$

3.6 Deterministic Factors

Mathematically speaking, the lodge has two main disturbances, on one hand the actual weather situation and on the other hand the number of guests at the lodge; all other disturbance inputs are a consequence of these two. For the calculations and simulations all external influences are assumed to be known, i. e., are determined for each time step before the simulation starts.
The important weather factors are the ambient temperature and the global irradiation; any wind influences are neglected. Based on the global irradiation the energy which can be gained by the PV cells and thermal solar collectors is calculated. For simplification the direct irradiation on the building, especially through the windowed staircase, is neglected. If an independency level of 90% for the lodge can be reached in the calculations without this additional heat, the independency level with it is even better.
For the power with which the guests support the lodge heating $100\frac{W}{p}$ is assumed (where p stands for *persons*) [22]. The volume flow rate of waste water is estimated around $2.1\frac{l}{h \cdot p}$, this rate is based on the maximum waste water volume of $6m^3$ per 120 persons and per day. [21].
Warm water for the guests to shower is provided, whenever there is enough heat. Warm water is also used for the kitchen and housekeeping. Because the warm water used to shower is a short-term load for the heat balance, the consumption is modeled with a usage profile over one day. It is a hygiene requirement that the employees take a shower every day. Because most of the guests leave the lodge before 7 am, 5 showers for the employees are planned from 8 to 9 am. The guests take their showers before or after dinner, from 6 to 8 pm or from 9 to 10 pm. Following the details provided by the SAC only 12.5% of the guests take a shower during their stay [17].
The amount of electricity needed by all the different devices, whose usage is based

on the occupancy of the lodge, is taken from the calculations of the Lucerne University [21]. The same source is used for the amount of electricity used by the house automation.

3.7 Data Source

As the start of construction of the lodge was in August 2008, no details about any parts of the lodge were set out at the moment the research was done. Some parameters are set based on information from one of the project partners, others are estimated according to one's best judgment. Details on each parameter can be found in *moroParameters.m* on the appended CD. The project partners are listed in Table 3.7.0.1.

Name	**Description**	**Project contribution**
Bearth & Deplazes Architekten AG	Architect's office	Executive architect's office
Center for Integrated Building Technology	Lucerne University of Applied Sciences and Arts	House automation project planning; overall component dimensioning
Feuron AG	Water tank manufacturer	Supplying the water tanks
KW Energie Technik e.K.	CHP manufacturer	Supplying the CHP
Lauber IWISA AG	Engineering company specializing in house automation	Detailed planning of the house automation
Muntwyler Energietechnik AG	Engineering company specializing in solar energy components	PV cell and power electronics dimensioning
Oerlikon Stationary Batteries Ltd.	Battery manufacturer	Supplying the Battery
Terralink GmbH	Engineering company specializing in water treatment	Supplying Waste water treatment plant

Table 3.7.0.1: Project Partners

Chapter 4

Modeling

The modeling process follows the theory mentioned in Section 2.1. First of all the system is analyzed concerning which parts have a storage in any form, afterwards every interaction between the lodge components and with the lodge is identified. Putting all together results in an interpretation of all interactions in the whole lodge, which the equations are based on. The whole model is energy based except the waste water tank which is a volume storage. This fact simplifies most connections to enthalpy and power flows.
Some components would not be turned on in the winter time. This is why the model is in the first place valid for the operating period in the summer, but with some adaptations it could be used for the winter period as well.

4.1 Storage Identification

To identify the different storages the functions of the lodge components have to be analyzed. The possible storages are the building mass, the different water tanks, the water fresh water supply, the thermal solar collectors, the CHP, the battery and the waste water treatment plant. Each storage is classified in one of the three classes: Fast, essential and slow dynamics. Based on this classification it is decided whether the storage can be neglected or has to be modeled as a state. In consideration of the later optimization the aim is to minimize the number of states as far as possible. The Table 4.1.0.1 shows the classifications for the storages.
All storage equations follow a lumped parameters approach.

4.2 Parts of the Model

In this section main parts of the model are introduced. Every description follows the same structure: First a short overview is given, then the different inputs into this part are explained and at last the complete mathematical relation is introduced. For every part a graph gives the main impression over the inputs and the state variables of this model part. The equations for every part are simplified to a certain point, nevertheless the reader should be able to follow the mathematical relations. All the equations are introduced as continuous, even though at the end they are implemented discretely. For more details on the implementation see the m-files on the appended CD.

Name	**Dynamics Class**	**Description**
Building	essential	Due to the ventilation, which distributes the energy in the building equally, the building is assumed as one energy storage.
Heating water tanks	essential	Because of the strong interconnection between the two tanks, they could be modeled as one, but the layered temperature arrangement implies a high and a low temperature storage (HTS / LTS). The temperature distribution over the two tanks is assumed as linear.
Warm drinking water tank	essential	Even though the energy level in the warm drinking water storage (WDWS) may drop fast, due to several showers taken at the same time, the storage is classified as 'essential'. Because other influences like the energy refill and the dependency on the number of people in the lodge are slower.
Fresh water supply	slow	Compared to the water tanks the mass of the fresh water supply is huge, hence its dynamics are negligible.
Thermal solar collectors	fast	Compared to the water tanks the water mass in the thermal solar collectors is very small. This results in fast energy dynamics.
CHP	fast	Even though the CHP is important for the problem, its dynamics are neglected.

Table 4.1.0.1: Storage classification.

4.2.1 Building

It is assumed that the energy distribution in the building is ideal due to the ventilation. That is why the building is modeled as one energy storage. The building is divided in three temperature zones, one is the bedrooms, the lounge area and the basement. How these zones are arranged is apparent in Figure 4.2.1.1. The lounge area is about 20% of the heatable building mass, the basement another 20% and the bedrooms build the rest of 60% . For the heatable building mass only the wood work of the floors from the basement to the third upper floor is considered, everything else is neglected. This results in a mass of $163.7t$. With the heat capacity of wood of $2.3\frac{kJ}{kg \cdot K}$ and the building average temperature range of $7°C$ to $21°C$ this gets to a storable energy amount of $5.2GJ$. The structure of the average building temperature is explained in Table 4.2.1.1.

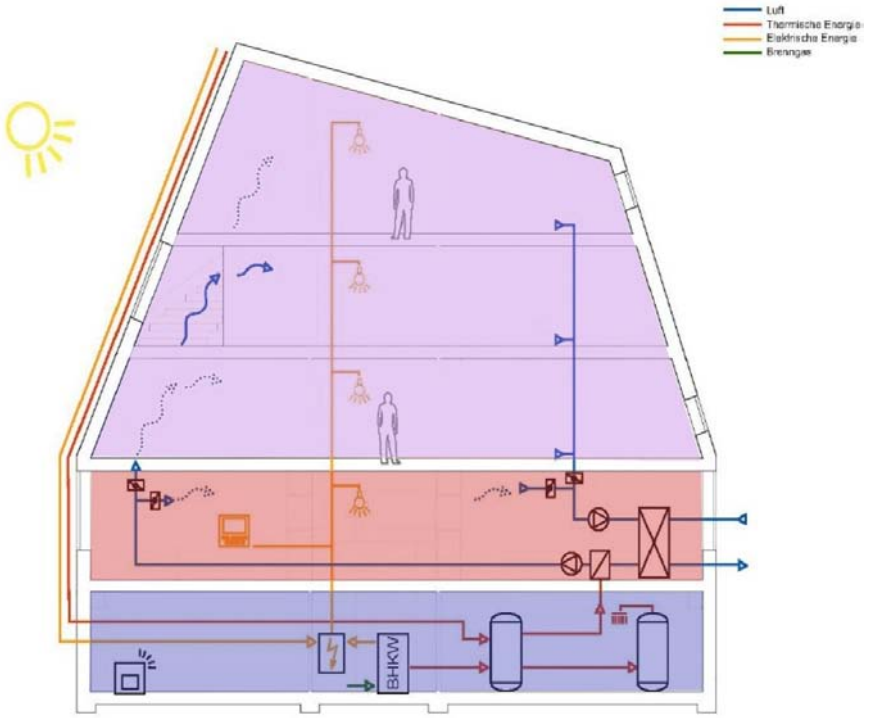

Figure 4.2.1.1: Building temperature zones, red: lounge/restaurant area, blue: basement and lilac: bedrooms.

	min	**aim**	**max**
Rooms 60%	$5°C$	$20°C$	$20°C$
Lounge 20%	$15°C$	$20°C$	$24°C$
Basement 20%	$5°C$	–	$20°C$
Building average	$7°C$	$15°C$	$21°C$

Table 4.2.1.1: Average building temperature structure.

Inputs and the Differential Equation In Figure 4.2.1.2 all the inputs to the building are apparent. The inputs to the building are the heat flows based on the following sources: the inhabitants, the heating system (HS), the ventilation, the environmental temperature and the solar irradiation.

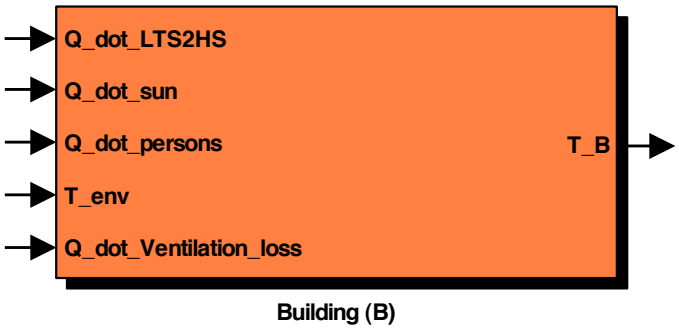

Figure 4.2.1.2: Block diagram of the building.

The data source for the environmental temperature and the heat radiated from the inhabitants is explained in Section 3.6. The environmental temperature determines the heat loss through the building hull due to heat conduction.

$$\dot{Q}_{B,loss} = (U_B \cdot A_B + U_W \cdot A_W) \cdot (T_B - T_{env}) \tag{4.1}$$

$\dot{Q}_{B,loss}$	Heat flow through the building hull
U_B	Heat conduction coefficient for the exterior walls
U_W	Heat conduction coefficient for windows
A_B	Environment temperature exposed area of the exterior walls
A_W	Area of the windows
T_B	Average building temperature
T_{env}	Environmental temperature

For the heating system it is assumed that all heat exchangers are designed well, i. e., the temperature difference of the outflows is assumed as zero. The heat transferred from the low temperature storage (LTS) to the building is calculated with the following enthalpy flow equation. This heat flow is added to the building energy and is subtracted from the LTS energy.

$$\dot{Q}_{LTS2HS} = ctr_{HS} \cdot c_{34} \cdot \eta_{HX,water-air} \cdot \dot{m}_{HS,max} \cdot (T_{LTS} - T_{VS}) \tag{4.2}$$

$\dot{Q}_{LTS2HS}$	Heat flow from the LTS to the Building
ctr_{HS}	Heating system control signal $\{0 \dots 1\}$
c_{34}	Heat capacity of water with a glycol concentration of 34%
$\eta_{HX,water-air}$	Heat exchanger efficiency for a water/air heat transfer, ideal = 1
$\dot{m}_{HS,max}$	Water mass flow rate [21]
T_{LTS}	Temperature of the water out of the LTS
T_{VS}	Temperature of the fresh air after energy recuperation

Because the windows cannot be opened by the guests but only by the warden the lodge has to be ventilated all the time. This ventilation system has a very good heat exchanger with an efficiency of 83%. The fresh air is already heated by a energy recuperation of the exhaust air before heated by the heating system.

$$T_{VS} = T_{env} + \eta_{HX,air-air}\,(T_B - T_{env}) \tag{4.3}$$

$$\dot{Q}_{ventilation,loss} = \dot{m}_{air} \cdot c_{air} \cdot (T_B - T_{VS}) \tag{4.4}$$

$\eta_{HX,air-air}$	Heat exchanger efficiency for a air/air heat transfer, 83% [19]
$\dot{Q}_{ventilation,loss}$	Heat loss through ventilation
c_{air}	Heat capacity of air, $1004.5\frac{J}{kg \cdot K}$
$\dot{m}_{air}$	Air mass flow rate [21]
T_B	Building temperature
T_{env}	Environmental temperature
T_{VS}	Temperature of the fresh air after energy recuperation

It is possible to include the influence of the solar irradiation on the building surface in the model, but due to missing information and no chance to measure it, it is neglected. If a high energy independency is reachable without consideration of the irradiation the result with consideration is even better.
For a better interpretation of the energy level in the storage a mean temperature for the storage is calculated:

$$T_B = \frac{Q_B + Q_{B,min}}{c_B \cdot m_B}. \tag{4.5}$$

Q_B	Useable heat in the building
$Q_{B,min}$	Energy level at the lower temperature bound
c_B	Heat capacity of the building (mainly wood), $c_{wood} = 2.3\frac{kJ}{kg \cdot K}$
m_B	Building mass, $163.7t$

With all these inputs the differential equation for the building is formulated:

$$\frac{d}{dt}Q_B = \dot{Q}_{LTS2HS} + \dot{Q}_{persons} + \dot{Q}_{sun} - \dot{Q}_{B,loss} - \dot{Q}_{ventilation,loss}. \tag{4.6}$$

$\dot{Q}_{persons}$	Heat radiated from the inhabitants
$\dot{Q}_{sun}$	Heat from solar irradiation on the building surface, in this calculation neglected, so set to 0

4.2.2 Warm Water Tanks

In the lodge there are physically three warm water tanks. The tank for the warm drinking water is modeled as a simple tank, but the two heating water tanks are modeled in a special way. These two tanks have a very strong horizontal interconnection, that is why they could be modeled as one. However, their structure implies a temperature layering. In the model this is taken into account by dividing both tanks horizontally in a high and a low temperature tank. The strong interconnection nevertheless allows to interpret the two physical tanks as one and to model one low and one high temperature storage. This approach is illustrated in Figure 4.2.2.1. As it can be seen in the plans on the appended CD the different heat exchangers in the warm water tanks are not of the same size. The lower heat exchangers are bigger than the upper one. Because of that and to assign in- and outlets properly to the separate storages the volume of the high and the low temperature tank is not equal.

Low Temperature Storage (LTS)

The low temperature storage represents the lower part of the two heating water tanks. The storable mass of water with a 34% glycol concentration is $2536kg$. Following the data of the pump specification from Lauber IWISA [14], this mixture has a density of $988\frac{kg}{m^3}$ (water at $50°C$) and a heat capacity of $3.6\frac{kJ}{kg \cdot K}$. The

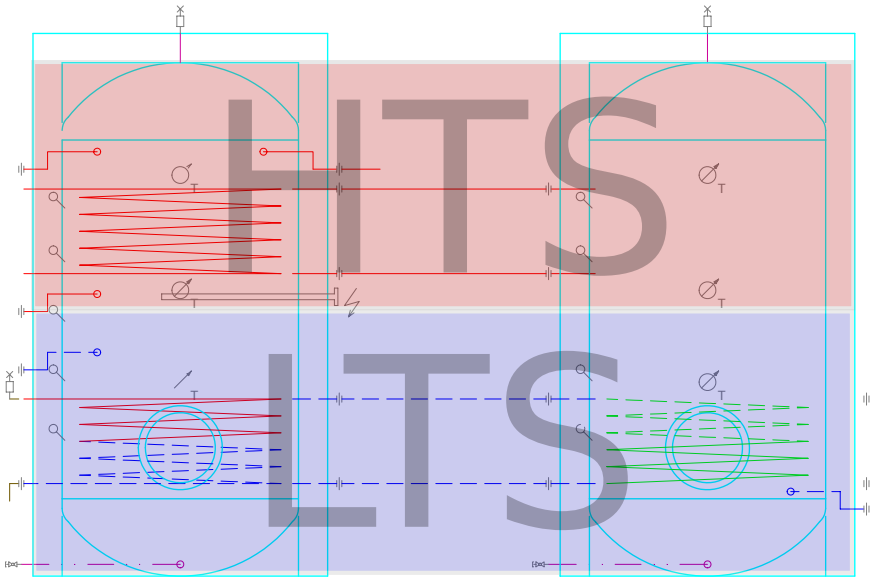

Figure 4.2.2.1: Split of the physical heating water tanks.

temperature reaches from $5°C$ to $80°C$ this results in a storable energy of $0.68GJ$. This limit of $80°C$ is set due to limited heat supply from the thermal solar collectors and cooling purposes for the CHP. Overheating can be prevented by heat evacuation to the fresh water supply.

Inputs and the Differential Equation of the LTS In Figure 4.2.2.2 all inputs into the low temperature storage are apparent. The LTS can be heated by the thermal solar collectors (TSC) and indirectly by the interaction with the high temperature storage (HTS). The energy level is reduced due to energy provided to the heating system and losses through heat conduction.

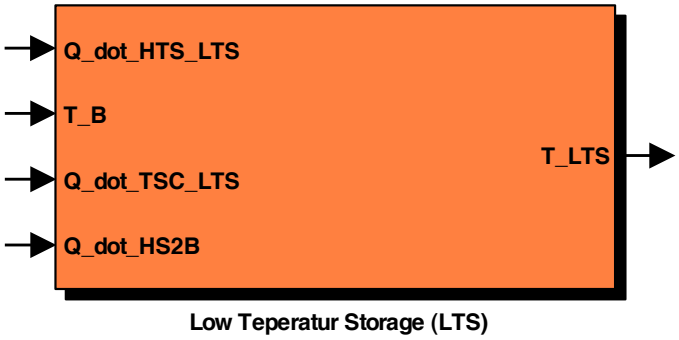

Figure 4.2.2.2: Block diagram of the low temperature storage.

$$\dot{Q}_{LTS,loss} = U_{LTS} \cdot A_{LTS} \cdot (T_{LTS} - T_B) \tag{4.7}$$

$\dot{Q}_{LTS,loss}$	Heat flow through the tank hull
U_{LTS}	Heat conduction coefficient for the tank hull
A_{LTS}	Building temperature exposed area of the tank hull
T_{LTS}	Average tank temperature
T_B	Building temperature

The energy supplied to the heating system is the same as in the equations for the building, only the sign in the differential equation is different (See Equation 4.2). The interconnection to the high temperature storage (HTS) is represented by the following equation:

$$\dot{Q}_{HTS\_LTS} = c_{HTS2LTS} \cdot m_{HTS} \cdot c_{34} \cdot \left(T_{HTS} - \frac{T_{HTS} \cdot m_{HTS} + T_{LTS} \cdot m_{LTS}}{m_{HTS} + m_{LTS}} \right), \quad (4.8)$$

where

$$c_{HTS2LTS} = \begin{cases} \frac{0.01}{3600} & ctr_{CHP} = 0 \\ \frac{50 \cdot 0.01}{3600} & ctr_{CHP} = 1 \end{cases}.$$

$\dot{Q}_{HTS\_LTS}$	Heat flow between the HTS and LTS
$c_{HTS2LTS}$	Heat exchange coefficient depending on ctr_{CHP}
c_{34}	Heat capacity of water with a glycol concentration of 34%
m_{HTS}	HTS heatable water mass
m_{LTS}	LTS heatable water mass
T_{HTS}	HTS average temperature
T_{LTS}	LTS average temperature

The Equation 4.8 represents a reduction of the temperature difference between the two tanks. The coefficient $c_{HTS2LTS}$ is an inverse time constant. The value $\frac{0.01}{3600}$ stands for $\frac{1}{100h}$. When the combined heat and power plant (CHP) is turned on, the heat flow between the two tanks is increased, because the cooling circle of the CHP pulls out water at the bottom of one of the physical tanks and puts it back in at the top of the other. This equation was developed to fit the assumption of a temperature layering in the water tanks.
The distribution of the energy provided by the thermal solar collectors is represented by the following simple equation. There are three heat exchangers (HX) connected to the thermal solar collectors, one in every water storage. Every HX can be disconnected separately. This fact allows the distribution of the energy there, where it is needed the most.

$$\dot{Q}_{TSC\_LTS} = ctr_{TSC\_LTS} \cdot \frac{\dot{Q}_{solar}}{\sum_i ctr_{TSC\_i}} \quad i = \{LTS, HTS, WDWS\} \quad (4.9)$$

$\dot{Q}_{TSC\_LTS}$	Heat flow form the TSC to the LTS
ctr_{TSC_i}	Control signal to connect and disconnect the TSC HX in the Tanks, $\in \{0, 1\}$
$\dot{Q}_{solar}$	Available energy

With all these inputs the differential equation for the LTS is formulated:

$$\frac{d}{dt} Q_{LTS} = \dot{Q}_{HTS\_LTS} + \dot{Q}_{TSC\_LTS} - \dot{Q}_{LTS2HS} - \dot{Q}_{LTS,loss}\,. \quad (4.10)$$

High Temperature Storage (HTS)

The upper part of the heating tanks is modeled as the high temperature storage. This storage has 34% glycol/water mixture capacity of $1812kg$ with the same characteristics as the LTS. This matches a storable energy amount of $0.48GJ$.

Inputs and the Differential Equation of the HTS The high temperature storage has inputs from the following sources: the TSC, the CHP, the electric heating and the interconnections to the other tanks (WDWS and LTS). See Figure 4.2.2.3. Of course this storage also suffers losses through the tank hull.

The equations for the TSC, the interconnection to the LTS and for losses are

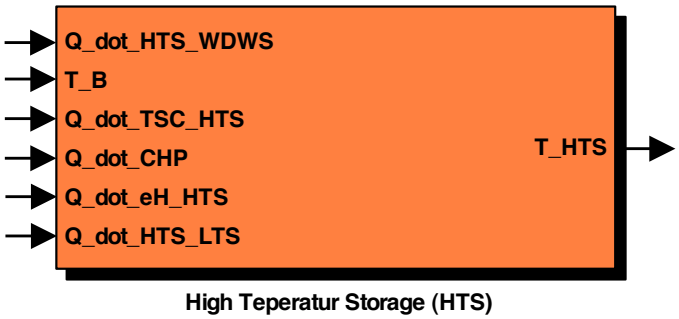

Figure 4.2.2.3: Block diagram of the high temperature storage.

analog to the equations of the LTS. See Equations 4.9, 4.8 and 4.7.
The equations for the CHP and the electric heating are very similar to each other and can be generalized the following way.

$$\begin{aligned} \dot{Q}_i &= c_i \cdot ctr_i \\ c_i &= \begin{cases} P_{eH,HTS,max} & \text{i=eH,HTS} \quad \text{electric heating} \\ \dot{Q}_{CHP,opt} & \text{i=CHP} \quad \text{combined heat and power (CHP)} \end{cases} \end{aligned} \tag{4.11}$$

$\dot{Q}_{CHP}$	Heat flow from the CHP
$\dot{Q}_{elec}$	Heat flow from the electric heating
ctr_{CHP}	CHP control signal
$ctr_{eH,HTS}$	Electric heating control signal

For the interconnection to the WDWS the following relation is applied. It has to be noticed that this interconnection is controllable by ctr_{HTS_WDWS}.

$$\begin{aligned} \dot{Q}_{HTS\_WDWS} &= ctr_{HTS\_WDWS} \cdot \dot{m}_{HTS\_WDWS,max} \\ &\quad \cdot c_{34} \cdot (T_{HTS} - T_{WDWS}) \end{aligned} \tag{4.12}$$

$\dot{Q}_{HTS\_WDWS}$	Controlled heat flow from the HTS to the WDWS
ctr_{HTS_WDWS}	Control signal for the connection between HTS and WDWS
$\dot{m}_{HTS\_WDWS,max}$	Mass flow in the interconnection between the HTS and WDWS [14]
c_{34}	Heat capacity of water with a glycol concentration of 34%
T_{HTS}	HTS average temperature
T_{WDWS}	WDWS average temperature

Then the differential equation for the HTS is

$$\begin{aligned} \frac{d}{dt} Q_{HTS} &= \dot{Q}_{TSC\_HTS} + \dot{Q}_{CHP} + \dot{Q}_{eH,HTS} \\ &\quad - \dot{Q}_{HTS\_LTS} - \dot{Q}_{HTS\_WDWS} - \dot{Q}_{HTS,loss} \,. \end{aligned} \tag{4.13}$$

Warm Drinking Water Storage (WDWS)

The third tank is the warm drinking water storage. Even though the tank has a small built in tank, it is modeled as one entire energy storage. It is assumed that the water, which refills the built in tank is heated immediately in a heat exchanger and thereby the energy level of the whole tank is affected. The 34% glycol/water mixture capacity of this storage is $1433kg$, the density, the heat capacity and the temperature limits are assumed to be the same as for the other two tanks. This results in a storable energy amount of $0.386GJ$.

Inputs and the Differential Equation of the WDWS An overview over the different inputs appears in Figure 4.2.2.4. The equations for the TSC, the connection to the HTS and the losses are analog to the Equations 4.9, 4.12 and 4.7 from the other water storages. The input $\dot{Q}_{warmDrinkingWater}$ is the external input for the warm water consumption depending on the number of people in the lodge. It is explained in Section 3.6.

The differential equation for the WDWS is the following

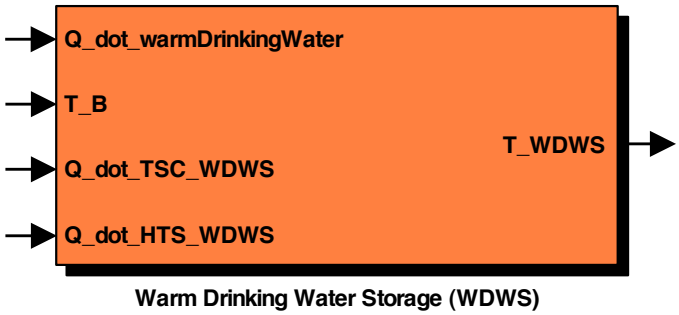

Figure 4.2.2.4: Block diagram of the warm drinking water storage.

$$\begin{aligned} \frac{d}{dt}Q_{WDWS} &= \dot{Q}_{TSC\_WDWS} + \dot{Q}_{HTS\_WDWS} \\ &\quad -\dot{Q}_{warmDrinkingWater} - \dot{Q}_{WDWS,loss}\,. \end{aligned} \tag{4.14}$$

4.2.3 Battery System

The fifth storage is the battery. In this model the battery, the power electronics and the grid are summarized in the "Battery System" block. This storage is also modeled as a pure energy storage, not all the conversions are modeled separately but are taken into account in the efficiency. The energy capacity of the battery is around $1GJ$, but to maintain a long life of the battery only 50% should be used. In the battery system different efficiencies are active, for details see Table 4.2.3.1.

Symbol	Value	Description
$\eta_{Battery}$	90.9%	Represents all processes from charging to discharging
$\eta_{PE,CHP}$	96%	Demodulation and conversion efficiency for the power from the CHP
$\eta_{PE,PV}$	99%	Conversion efficiency for the power from the PV
$\eta_{PE,load}$	94%	Conversion efficiency for the power to the load

Table 4.2.3.1: Battery System efficiencies, these numbers resulted from the fact sheets about the components or from personal discussions with the manufacturer.

The Differential Equation An overview of the in- and outputs of the battery system is shown in Figure 4.2.3.1. The mathematical representation is relatively simple and is shown by the following equation.

$$\begin{aligned} \frac{d}{dt}E_{SOC} &= \eta_{Battery} \cdot (\eta_{PE,CHP} \cdot P_{CHP} + \eta_{PE,PV} \cdot P_{PV}) - \\ &\quad \frac{1}{\eta_{PE,load}} \cdot (P_{WWTP} + P_{stoch} + P_{HA} + P_{eH\_HTS} + P_{HA}) \end{aligned} \tag{4.15}$$

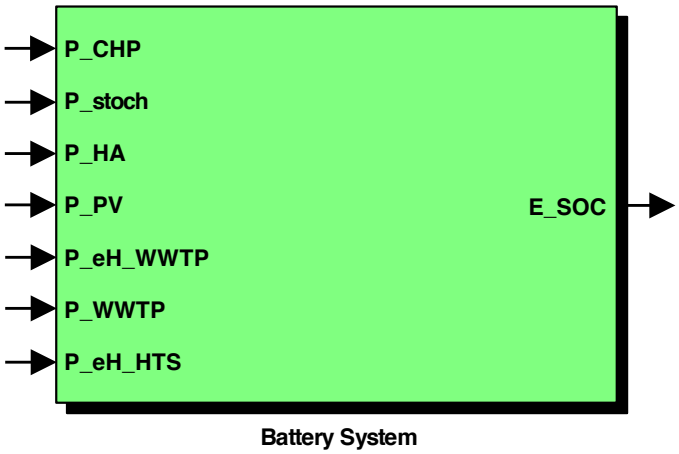

Figure 4.2.3.1: Block diagram of the battery.

$\frac{d}{dt}E_{SOC}$	Variation of the state of charge of the battery
P_{CHP}	Power provided by the CHP [8]
P_{PV}	Power provided by the PV [21]
P_{WWTP}	Power used for the WWTP, see Equation 4.17.
P_{stoch}	Power used for the stochastic load [21]
P_{eH_HTS}	Power used for the electric heating of the HTS [10]
P_{eH_WWTP}	Power used for the electric heating in the WWTP room, neglected and set to 0 in this thesis.
P_{HA}	Power used for the house automation [21]

4.2.4 Waste Water Treatment Plant (WWTP)

As last and probably the simplest storage there is the tank of the waste water treatment plant. This is a volume storage with a capacity of $5.5m^3$. The filling of the tank is dependent on the number of people in the lodge. There is a control signal which controls the operating of the treatment plant. In this model this control signal is simplified to an on/off switch. In a further step it will have to be taken into account that the plant cannot always be turned off immediately. The configuration of this storage is apparent in Figure 4.2.4.1. As the volume flow to the WWTP is

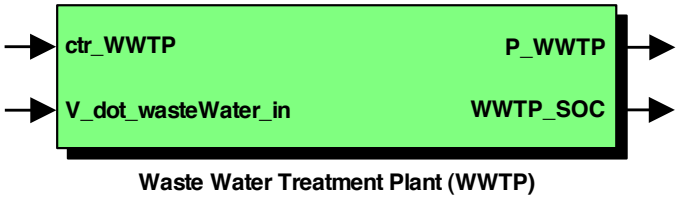

Figure 4.2.4.1: Block diagram of the waste water treatment plant.

directly dependent on the number of people in the lodge and the other input is the control input (which is 1 or 0), the differential equation is formulated directly.

$$\frac{d}{dt}WWTP_{SOC} = \frac{\dot{V}_{ww,in} - ctr_{WWTP} \cdot \dot{V}_{clw,out}}{V_{WWTP,max}} \tag{4.16}$$

$\frac{d}{dt}WWTP_{SOC}$	Variation of the state of charge of the WWTP tank
$V_{ww,in}$	Inflow of waste water, $\dot{V}_{ww_{per\_person}} \approx 2\frac{l}{person \cdot h}$
$\dot{V}_{clw,out}$	Waste water cleaning rate $\frac{5.5m^3}{14h} \approx 0.4\frac{m^3}{h}$ [15]
ctr_{WWTP}	WWTP control signal

The second output of this block is the power consumption of the waste water treatment plant.

$$P_{WWTP} = P_{WWTP_{standby}} + ctr_{WWTP} \cdot P_{WWTP_{on}} \tag{4.17}$$

P_{WWTP}	Power consumption of the WWTP
$P_{WWTP_{standby}}$	Standby power consumption [15]
$P_{WWTP_{on}}$	Additional power consumption when the WWTP is turned on [15]

4.2.5 Entire Model

By putting all these components together the entire model is obtained. This model is visualized in Figure 4.2.5.1. All blocks with a shadow represent a differential equation; all the other blocks are algebraic relations. The model has 8 control inputs (blue) and 10 deterministic inputs (yellow). The outputs are 6 state variables (red) and the fuel consumption (magenta) which is important for the optimization. The model parts can be grouped in 3 different groups: thermal (salmon), electric (green) and the combination of both (brown). This subdivision will be important for later optimization, which treats the two groups, thermal and electric, separately.

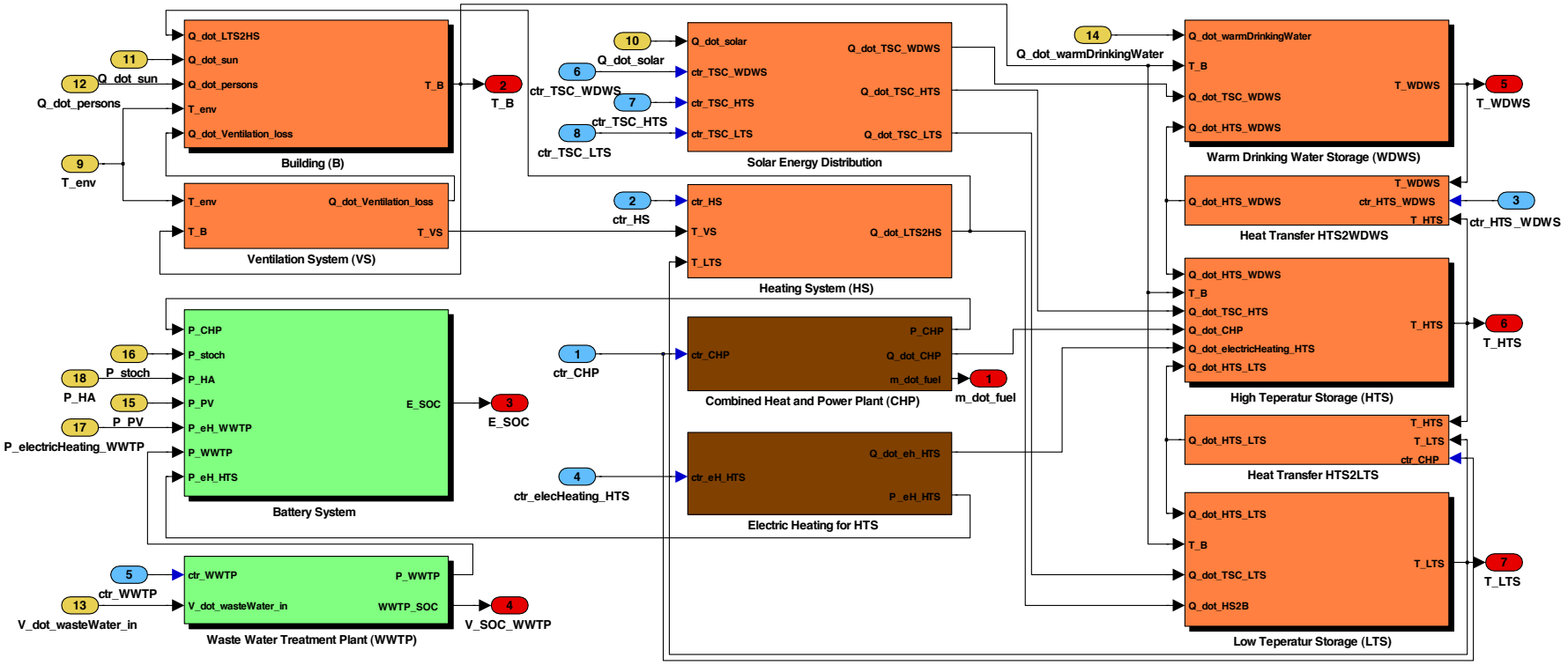

Figure 4.2.5.1: Block diagram of the entire model.

4.3 Model Verification

To verify the model it is split into its elementary parts. To verify each equation some input and initial values are set and the output value is calculated. In addition, at least one simple scenario has been created for each part to test empirically if the results are plausible. These scenarios are discussed here briefly.
A few tests take their input data for outside temperature, solar irradiation etc. from an exemplary week with average weather conditions and a weekend with 120 visitors in the middle (datasource: [21]).

4.3.1 Battery

For this test the exemplary week was used. The results are plotted in Figure 4.3.1.1.

Input Signals

$P_{eH\_WWTP} = 0$	Energy used to heat the WWTP room.
$P_{eH\_HTS} = 0$	Energy used to heat the HTS.
P_{WWTP}, P_{stoch}, P_{PV}, P_{HA}	These values are taken from the exemplary week.
$P_{CHP} = 0$	The CHP is turned off.

Output Signals

E_{SOC}	State of charge of the battery over time.
P_{WWTP}	Power consumed by the WWTP.

Initial Values

$$E_{SOC,0} = 90\% \text{ of } E_{SOC,max} = 932MJ$$
$$V_{wasteWaterTank\_SOC,0} = 0.5 \cdot V_{wasteWaterTank\_SOC,max} = 2.75m^3$$

Simulation Results

As Figure 4.3.1.1 shows, the E_{SOC} never falls below about 58%, whereas 50% is the tolerable minimum value. E_{SOC} fell from 90% to 77% in one week. Considering that in the exemplary week the weather is average and the number of visitors is high, this is a realistic result.

4.3.2 WWTP

The results are plotted in Figure 4.3.2.1.

$\dot{V}_{wasteWater\_in} = 50l$ per person and 24 hours	120 persons are in the building.
ctr_{WWTP}	Control signal, turns the treatment process on and off.

Output Signals

$V_{wasteWaterTank\_SOC}$	Waste water tank level over time.
P_{WWTP}	Power consumed by the WWTP.

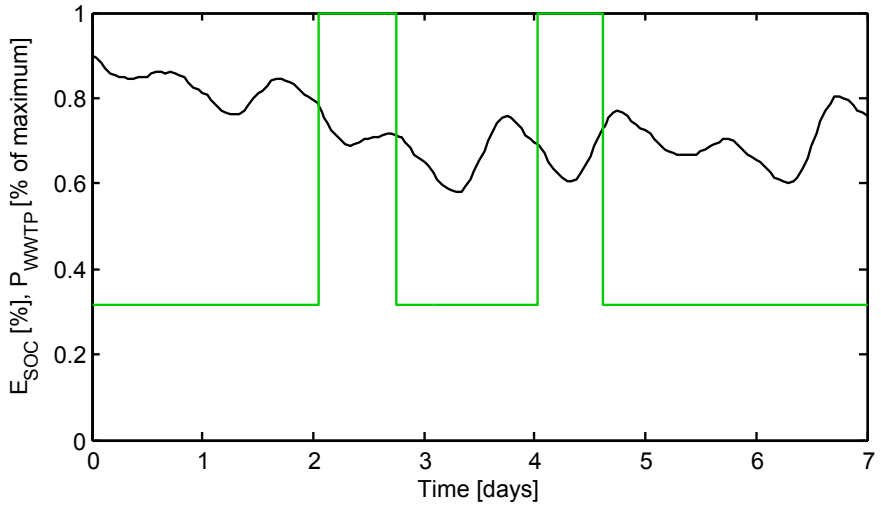

Figure 4.3.1.1: Battery simulation:
black: $E_{SOC}[\%]$ Energy stored in the battery
green: $P_{WWTP}[\%]$ Energy consumed by the WWTP: When it is turned on, it consumes $2.19kW$, when it is in standby mode it uses roughly $700W$.

Initial Values

$V_{wasteWaterTank\_SOC,0} = 0$	The tank is empty at the begin of the simulation.

Simulation Results

After 18 hours the tank is almost full and the WWTP is turned on. From then on the maximum amount of energy is needed to treat the water.

4.3.3 Building

For this test the exemplary week was used also. The results are plotted in Figures 4.3.3.1 and 4.3.3.2.

Input Signals

$T_{env} = -7°C$	Environment temperature
$\dot{Q}_{persons} = 120 \cdot 100$	120 persons, $\frac{100W}{person}$
$\dot{Q}_{HS2B} = 0$	The heating system is turned off.
$\dot{Q}_{sun} = 0$	No solar irradiation into the stairways takes place.

The ventilation losses are calculated out of the heat exchanger efficiency and the difference between the building and the outside temperature.

Output Signals

T_B	Mean temperature of the building over time

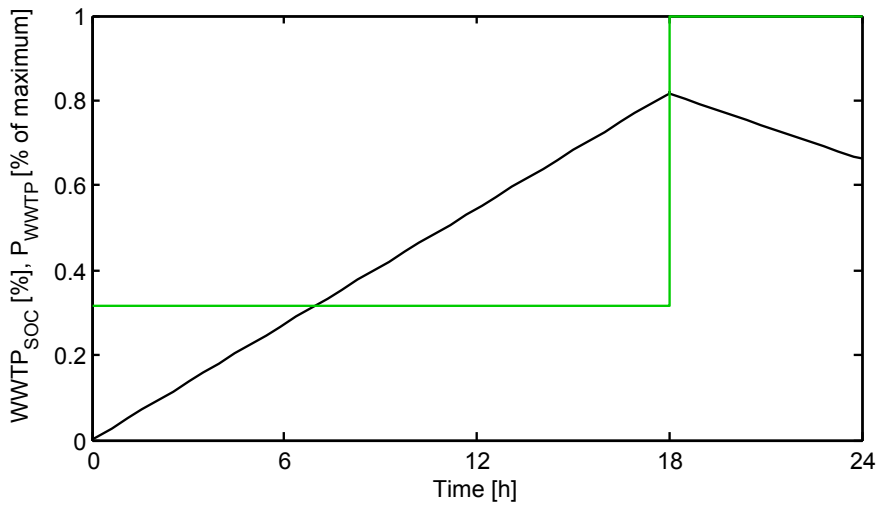

Figure 4.3.2.1: WWTP simulation:
black: $V_{wasteWaterTank\_SOC}[\%]$ SOC of the waste water tank
green: $P_{WWTP}[\%]$ Energy consumed by the WWTP: When it is turned on, it consumes $2.19kW$, when it is in standby mode it uses roughly $700W$.

Initial Values

$T_{B,0} = 7°C$	Initial building temperature

Simulation Results

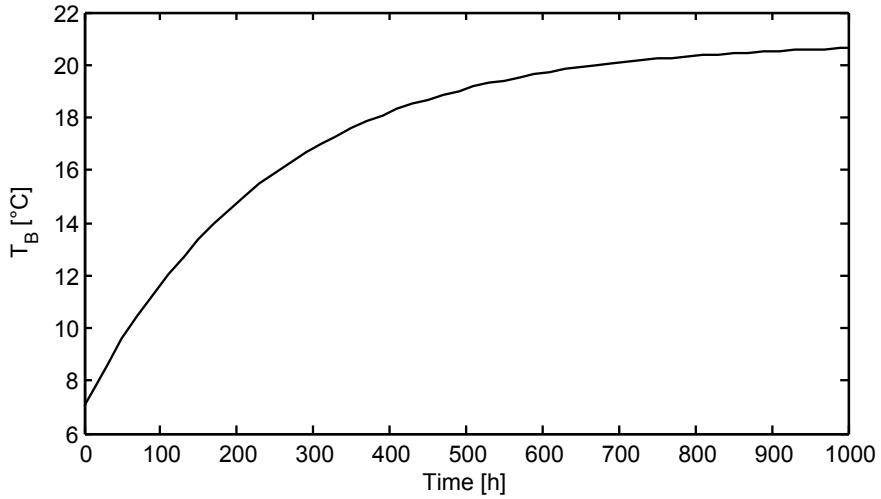

Figure 4.3.3.1: Long-term simulation of the building:
black: $T_B[°C]$ Temperature of the building

The building itself is a first order system, i. e., T_B converges towards a finite value. As in Figure 4.3.3.1 can be seen the final value is around $21°C$, which is pretty warm.
However, the 120 persons are only at night inside the building, i. e., for maximum 10 hours. In this time period the mean temperature of the building increases more than $0.5°C$, which is notable (see Figure 4.3.3.2).

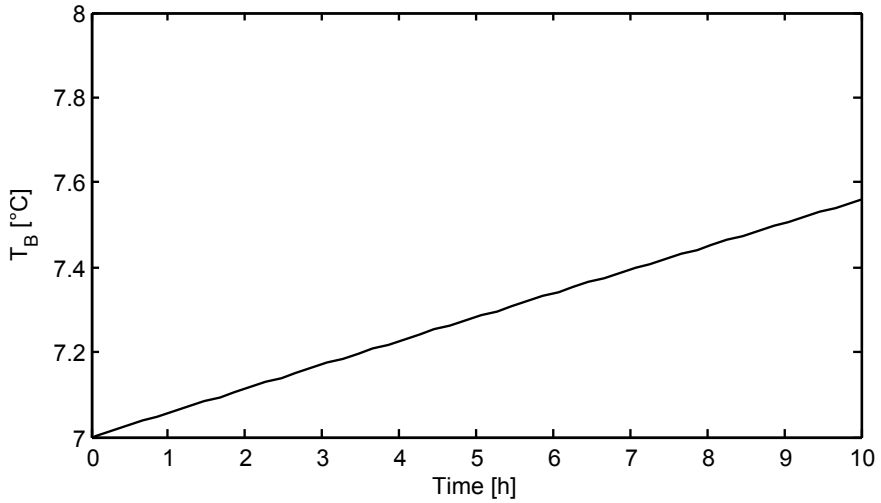

Figure 4.3.3.2: Short-term simulation of the building:
black: $T_B[^\circ C]$ Temperature of the building during one night

4.3.4 LTS, HTS & WDWS

The three heating tanks were first tested separately. Each tank is a first order system and the inputs are simply added up.
What is shown here is a simulation, where all tanks are connected and interact. A very big influence on the behavior has $c_{HTS2LTS}$, which is the inverse heat exchange time constant between the LTS and the HTS. The same simulation was repeated with varying $c_{HTS2LTS}$ to determine a realistic behavior, so $c_{HTS2LTS}$ could be chosen correctly.
For these simulations the exemplary week was used. The results are plotted in Figures 4.3.4.1, 4.3.4.2, 4.3.4.3 and 4.3.4.4.

Input Signals

$\dot{Q}_{TSC\_WDWS} = 0W$	No heat is transferred from the TSC to the WDWS.
$\dot{Q}_{TSC\_HTS} = \dot{Q}_{TSC\_LTS}$	The incoming heat is split up between HTS and LTS.
$\dot{Q}_{HTS\_WDWS}$	Heat is transferred, if $T_{HTS} > T_{WDWS}$ and $T_{HTS} > 50^\circ C$.
$\dot{Q}_{warmDrinkingWater}$	Warm drinking water consumption of the HA and the visitors: The input vector is from the exemplary week.
$\dot{Q}_{solar}$	Energy generated by the thermal solar collectors: The input vector is from the exemplary week.
$T_B = 8^\circ C$	Target temperature for the building

$\dot{Q}_{LTS2HS}$	Heat, which is transferred from the LTS to the building: This value is set to 16% (where $T_{LTS} - T_B = 30°C$) of the maximum mass flow, which is equivalent to $1.5kW$ heating power. This is in the same order of magnitude as the effective heating power demand.
$\frac{1}{3600 \cdot c_{HTS2LTS}} = [10, 50, 100, 500]$	Time constant in hours
$ctr_{CHP} = ctr_{eH,HTS} = 0$	Neither the CHP nor the battery heats the HTS.
$\dot{Q}_{HTS\_LTS} \sim c_{HTS2LTS}$	$\dot{Q}_{HTS\_LTS}$ is proportional to $c_{HTS2LTS}$ (see Equation 4.8).

Output Signals

T_{WDWS}	Temperature of the WDWS over time
T_{HTS}	Temperature of the HTS over time
T_{LTS}	Temperature of the LTS over time

Initial Values

$Q_{WDWS,0} = Q_{HTS,0} = Q_{LTS,0} = 0.5$	The temperatures of the WDWS, HTS and LTS tank are initially at $42.5°C$.

Simulation Results

In the first three days the weather is bad. That causes the LTS to cool down below $20°C$. In reality, the CHP would supply the tank with heat, before it reaches such a critical level, where it is not able to heat the building anymore.
During the second half of the simulation period, the weather is good, so the HTS reaches its maximum at $80°C$ and heats up the WDWS.
Figures 4.3.4.1 to 4.3.4.4 show the big influence of $c_{HTS2LTS}$. The more this constant decreases, the less the HTS reacts on the run of the LTS. This causes the HTS to keep its heat, while the LTS cools down dramatically. Notice, that distribution of the thermal solar energy is held constant: One half of the energy is fed into the LTS and the other half into the HTS, although the LTS needs much more heat than the HTS.
Considering these results a time constant $\frac{1}{c_{HTS2LTS}} = 100$ hours (i. e., $c_{HTS2LTS} = \frac{0.01}{3600}$) was chosen. One exception was made: When the CHP is turned on, the time constant is reduced to 2 hours, because the CHP sucks cooling water in from the LTS and gives the heated up water to the HTS at $80°C$. This causes a strong mixing of the heating water of both tanks.

4.4 Model Validation

The model could not be validated, because the lodge is not built yet. No similar buildings exist, which could have been used as a surrogate.

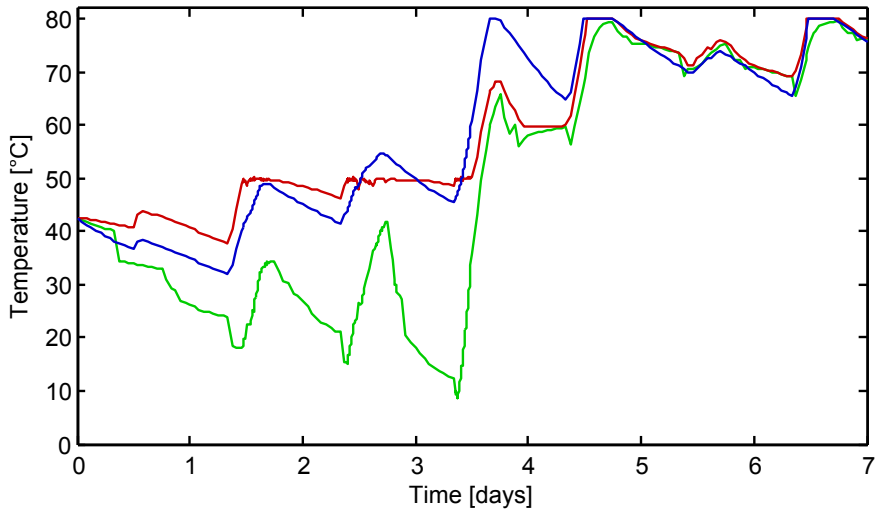

Figure 4.3.4.1: Simulation of the heating system with $\frac{1}{c_{HTS2LTS}} = 10h$:
green: $T_{WDWS}[^{\circ}C]$ Temperature of the WDWS
blue: $T_{LTS}[^{\circ}C]$ Temperature of the LTS
red: $T_{HTS}[^{\circ}C]$ Temperature of the HTS
The time constant $\frac{1}{c_{HTS2LTS}}$ is set to 10 hours. The HTS follows every move of the LTS. This is not realistic in a tank where a layering is part of the concept.

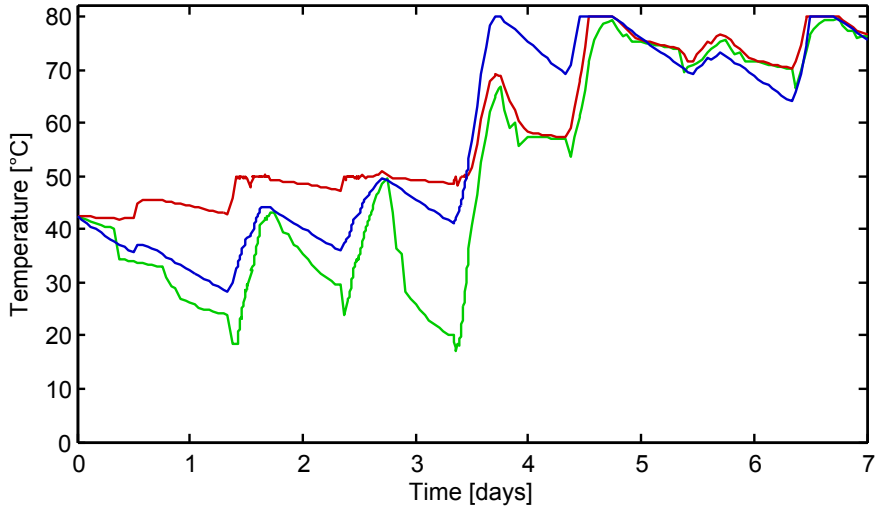

Figure 4.3.4.2: Simulation of the heating system with $\frac{1}{c_{HTS2LTS}} = 50h$:
green: $T_{WDWS}[^{\circ}C]$ Temperature of the WDWS
blue: $T_{LTS}[^{\circ}C]$ Temperature of the LTS
red: $T_{HTS}[^{\circ}C]$ Temperature of the HTS
The time constant $\frac{1}{c_{HTS2LTS}}$ is set to 50 hours.

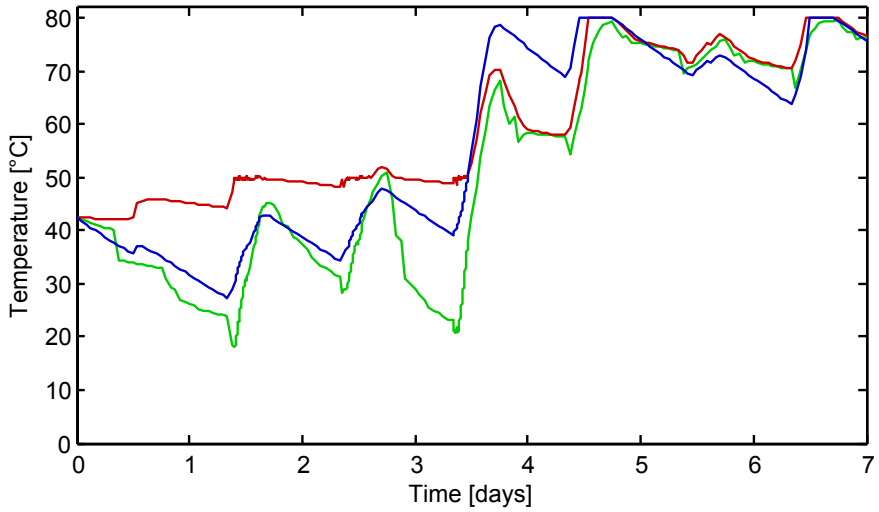

Figure 4.3.4.3: Simulation of the heating system with $\frac{1}{c_{HTS2LTS}} = 100h$:
green: $T_{WDWS}[^\circ C]$ Temperature of the WDWS
blue: $T_{LTS}[^\circ C]$ Temperature of the LTS
red: $T_{HTS}[^\circ C]$ Temperature of the HTS
The time constant $\frac{1}{c_{HTS2LTS}}$ is set to 100 hours. The HTS still follows the moves of the LTS, but very moderate. The time constant has to be chosen somewhere between 50 and 100 hours.

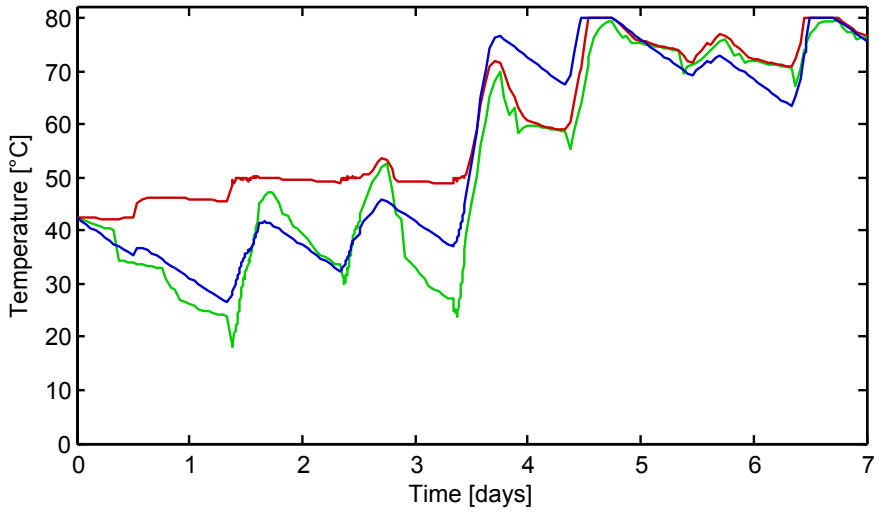

Figure 4.3.4.4: Simulation of the heating system with $\frac{1}{c_{HTS2LTS}} = 500h$:
green: $T_{WDWS}[^\circ C]$ Temperature of the WDWS
blue: $T_{LTS}[^\circ C]$ Temperature of the LTS
red: $T_{HTS}[^\circ C]$ Temperature of the HTS
The time constant $\frac{1}{c_{HTS2LTS}}$ is set to 500 hours. The HTS does not follow the moves of the LTS anymore, it behaves almost independent. A time constant of 500 hours is too large.

Chapter 5

Optimization

5.1 Derivation of the Optimization Modality

5.1.1 Structure of the Problem

To find a control signal which minimizes the fuel consumption of the entire system the optimization methods LP and DP are used. With a LP the global minimum of a convex function with affine constraints is calculated. As the system description enters as a constraint to the problem a necessary condition is that the system is linear. This was only the case in the subsystem containing the battery and the WWTP, referred to as *electric cycle*. The *thermal cycle*, consisting of the WDWS, HTS, LTS and the mass of the building, has several non-linear connections. This is mainly because the in- and outputs of each component are heat flows, which depend on the state (i. e., temperature) multiplied by the control input (i. e., mass flow). Calculating the entire system using DP was not possible, either. A DP grows exponentially with the number of state variables of the problem. The current standard hardware is not sufficient to calculate a solution with a DP including all six state variables of the system in a reasonable amount of time.

5.1.2 A Promising Idea

Considering the conditions mentioned above, the idea of dividing the system into a linear and a nonlinear part was promising. The solution of the linear part, consisting of the elements of the electric cycle, could then be found with a LP. The solution of the nonlinear part, i. e., the thermal cycle, could be obtained by solving a DP. The optimal solution could then be determined by combining the solutions of the sub problems.

5.1.3 Is a Separation of the Problem Possible?

In fact only two signals interconnect the thermal and the electric cycle: the CHP, which always produces heat and electric energy simultaneously, and the "electric heating" where the battery dissipates energy into the HTS (see Figure 4.2.5.1).

4 Different Interaction Cases

In the following paragraph all four possible interaction cases between the two parts of the system are analyzed. For each case it is to show how a desired action in one part of the system would affect the other part in reality (e. g., the electric cycle wants to dissipate energy from the battery; this causes a temperature increase in

the HTS). This implies consequences of the missing communication between the two parts in the simulation. The behavior has to be analyzed in the time span starting at the desired interaction and ending at the end of the simulation (e. g., what is the effect if the HTS temperature does not increase in the simulation although it would so in reality; how does this affect the optimality of the solution).

Case 1: The *CHP* is turned on due to the *lack of electric energy*

Reality	**Split System**
In reality the CHP provides the battery with electric energy and the heating tanks with thermal energy simultaneously. HTS and LTS can always take up heat, because the LTS is connected to the fresh water supply where compared to the modeled system almost an infinite amount of heat can be stored.	In the split system the CHP generates electric power if the demand comes from the electric cycle. The simultaneously produced heat is not considered in the calculation of the thermal cycle. This is a valid conservative assumption: the fuel consumption calculated in the simulation might be higher than the fuel consumption in reality.

Case 2: The *CHP* is turned on due to the *lack of thermal energy*

Reality	**Split System**
As mentioned in Case 1 the CHP provides the battery with electric energy and the heating tanks with thermal energy simultaneously. In case the battery is already fully charged, it could dissipate only $3kW$ of the incoming $12kW$ into the HTS and LTS. Therefore the CHP could not work with full load. What implies a suboptimal solution.	In the split system the CHP generates thermal power if the demand comes from the thermal cycle. The simultaneously produced electric power is not considered in the optimization of the electric cycle. Therefore the overall fuel consumption might be higher than in reality.

Example on Case 1 & 2 Consider the situation, where there is a lack of electric energy. The CHP is activated immediately in the LP (which optimizes the electric cycle) for one hour. Because there is no connection to the thermal cycle, the DP (which computes the optimal control inputs for the thermal cycle) does not take into account the coproduced heat. Assume a lack of thermal energy at a later point in time. The CHP is then activated in the DP for one hour, the LP does not take the coproduced electricity into account, however. The overall fuel consumption is then the sum of the fuel used by the DP and by the LP which is in this case the consumption of the CHP during two hours, although the energy considered in the calculation is one hour CHP. In reality, the coproduced heat during the first hour might have been enough, such that the CHP would not have to be activated a second time. The overall fuel consumption would be the consumption of one hour.

Case 3: *Electric heating* is turned on due to *excess of electric energy*

Reality	Split System
In reality the battery dissipates energy into the HTS, i. e., E_{SOC} decreases by $3kW$ and Q_{HTS} increases by $3kW$. Electric heating can always be activated by the electric cycle, because it is assumed that the thermal cycle is always able to store additional heat.	In the split system the battery is allowed to dissipate energy, the energy gained in the HTS is not considered, however. This case is similar to Case 1.

Case 4: *Electric heating* is turned on due to a *lack of thermal energy*

Reality	Split System
In reality the battery dissipates energy into the HTS, i. e., E_{SOC} decreases by $3kW$ and Q_{HTS} increases by $3kW$. However, the electric cycle is not always able to provide heat. Therefore, electric heating can only be activated by the thermal cycle if certain conditions are fulfilled.	In the split system it is not clear, whether the battery is able to supply the heating tanks with thermal energy. Therefore, to obtain a reasonable solution, the electric heating option is disabled ($ctr_{eH\_HTS} = 0$) in the DP, i. e., the thermal cycle cannot request energy from the electric one.

Summary In all four Cases some sort of iteration including LP and DP is needed to find a control signal which is optimal for the entire system. This optimal control signal though is not guaranteed to be globally optimal. However, an iteration algorithm is not implemented in this thesis out of the following reason: If it turns out that the thermal cycle does not use any fuel at all during a certain period, the maximal grade of autarky can be calculated without an iteration. As the results show this is usually the case.
In the other case, if the electric cycle is autark but the thermal cycle needs energy from the CHP, the calculated grade of autarky is almost the achievable maximum. This is because the energy from the CHP into the thermal cycle might be substituted by energy from the battery which is fed by eletric heating into the thermal cycle. However, the results show that the amount of energy, which can be shifted from the electric to the thermal cycle, is quite small.
If both cycles need fuel in the same time period, the estimation of the grade of autarky is not straight forward, only an iterating algorithm can provide a meaningful result.
Following the arguments discussed above one can conclude, that the problem is dividable indeed, although certain restrictions have to be taken into account in order to derive a meaningful result.

Besides these two programs a heuristic controller was designed which is described in Section 5.4. It was used firstly to get an idea of what the solution could look like and secondly as a reference to the optimized solution. The heuristic controller acted on the entire system, i. e., the system was not split.

5.2 Linear Program

This section illustrates the *implementation* of the LP and follows strictly the code of the m-files *lp_init.m* and *lp_calc.m* on the appended CD. In *lp_init.m* the program is initialized, then *lp_calc.m* is called which manipulates the matrices and calls the

numeric optimizer provided by MATLAB®. Finally *lp_plot.m* is called to visualize the results. The theoretical basics are explained in Chapter 2.4.

5.2.1 Initialization of the LP

The corresponding code is in the m-file *lp_init.m*, which can be found on the CD.

1. The start and end dates of the simulation are defined
2. The linear part of the system consisting of the battery and the WWTP, is extracted from the Simulink® model and written in matrix form. This is done with the MATLAB® function called *dlinmod* [1].
   Furthermore, the sampling time is fixed and the routine *moroParameters.m* is loaded, which contains all system parameters. This routine automatically returns the determined inputs for this time sequence.
3. The simulation horizon is calculated based on the start and the end dates. Then, the weighting vectors are defined. Only the CHP and the electric heating control input are weighted. (Switching on the electric heating is punished to keep a maximum amount of energy in the electric cycle. If this input would not be punished, the optimized solution would act arbitrarily at the end of the optimization horizon.)
   An optimized input vector never switches CHP and electric heating on at the same time. Therefore the weights can be arbitrary but positive.
4. The input and state bounds are defined. The waste water tank is allowed to assume any state from empty to entirely full. The battery must not have a SOC under 50% for technical reasons. The inputs are normalized and therefore limited to values between 0 and 1. For the determined inputs the upper limit is chosen sufficiently larger than the largest determined value.
5. The initial and the final states are set. The final state condition is an equality condition; if the final state cannot be reached for some reason, the linear program becomes unfeasible.
6. The m-file *lp_calc.m* is called (see Section 5.2.2) which returns a vector Z which contains all input and state trajectories over time
7. The input, output and state components are renamed and the entire workspace is saved.

5.2.2 Transformation of the Given Information into Equality and Inequality Constraints

The corresponding code is in the m-file *lp_calc.m*, which can be found on the CD. The code transforms all user-defined conditions into a LP. The corresponding theory is found in 2.4.4.
Like mentioned in the theory, the LP can be written in a simplified way, if all control inputs and state vectors have positive entries only. This is indeed the case for the conditions discussed above. The simplification reduces computational time and memory usage dramatically.
The matrices containing all inequality and equality constraints are visualized in Figures 5.2.2.1 and 5.2.2.2 to help the reader understanding the structure.
In a next step, these matrices are handed over to the *linprog* algorithm of MATLAB®,

[1] dlinmod obtains linear models from systems of ODEs and discrete-time systems.
$[A, B, C, D] = dlinmod('SYS', TS)$ obtains a discrete-time state-space linear model with sample

$$A_{ineq} \cdot Z \leq B_{ineq}$$

$$\begin{bmatrix} \varepsilon_x & 0 \\ 0 & \varepsilon_u \end{bmatrix} \cdot \begin{bmatrix} X \\ U \end{bmatrix} \leq \begin{bmatrix} F_x \\ F_u \end{bmatrix}$$

Figure 5.2.2.1: Inequality constraints: The sub matrices are implemented this way in *lp_calc.m* which can be found on the appended CD.

$$A_{eq} \cdot Z = B_{eq}$$

$$\begin{bmatrix} \begin{bmatrix} I\text{-}A_{cal,cross} \end{bmatrix} & \begin{bmatrix} -B_{cal,cross} \end{bmatrix} \\ \begin{bmatrix} O \end{bmatrix} & \begin{bmatrix} S \end{bmatrix} \\ \begin{bmatrix} A_{final} \end{bmatrix} & \end{bmatrix} \cdot \begin{bmatrix} X \\ U \end{bmatrix} = \begin{bmatrix} \begin{bmatrix} H_{cal} \cdot x_0 \end{bmatrix} \\ \begin{bmatrix} D \end{bmatrix} \\ \begin{bmatrix} B_{final} \end{bmatrix} \end{bmatrix}$$

Figure 5.2.2.2: Equality constraints: The sub matrices are implemented this way in *lp_calc.m* which can be found on the appended CD.

which computes the solution of the linear program (see Chapter 2.4.5) and returns vector $Z = (X^T \quad U^T)^T$ to *lp_init.m*.

5.2.3 Frequent Errors

When executing *lp_init.m* the following errors occur now and then. They are documented below.

- Out of memory: The LP needs a great amount of memory during the preparation of the matrices, i. e., in parts 1, 2 and 3 of *lp_calc.m*. The linprog® algorithm called in part 4 does not need a lot of memory resources.
  If this error occurs the length of the simulation should be decreased. On a personal computer a simulation up to three weeks works well, on a workstation a simulation with a time horizon up to 6 or 7 weeks can be computed.

- linprog® terminates because problem is infeasible: If this error occurs a small variation of the initial (and final) condition or a small shift in the time period is often sufficient to obtain a feasible solution.

5.3 Dynamic Programming

This section explains how the dynamic programming algorithm, which is explained in Section 2.3), is applied on the thermal subsystem. To retrieve the plotted result the algorithm is divided in three consecutive processes:

- **Backward optimization**
- **Forward evaluation**
- **Plotting**

time TS of the system of mixed continuous and discrete systems described in the block diagram $'SYS'$ {...}. (Citation from the MATLAB® help)

For a process and file overview see Figure 5.3.0.1. The first two processes are explained in the following sections. The explanation concentrates on points which are not evident from the code and its comments. All the processes can be started by cell-by-cell evaluation of the file *dp.m*. All files mentioned here can be found on the appended CD. This section follows these files entirely, a parallel look at the files can be helpful.

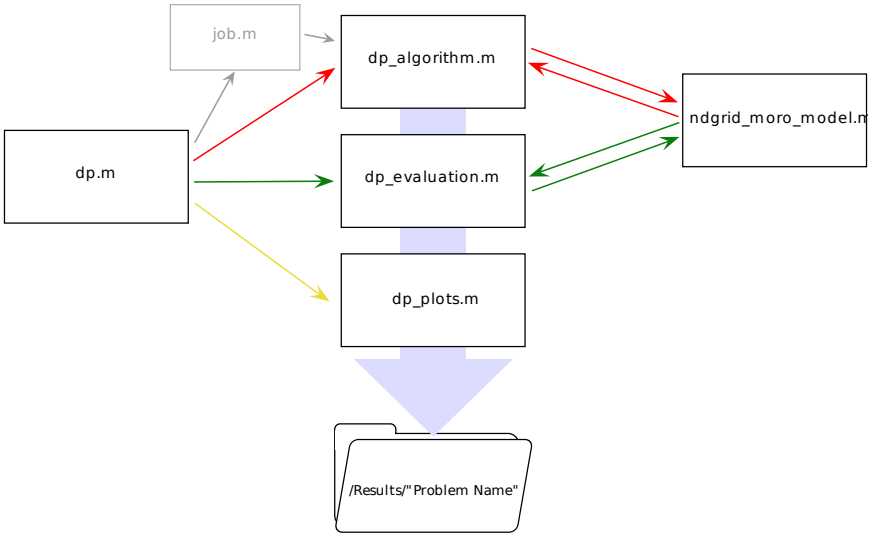

Figure 5.3.0.1: Connections of the separate m-files.
red: Backward optimization
green: Forward evaluation
yellow: Plotting
gray: optional path to run on a server

5.3.1 Backward Optimization

Initializing

1. After the file *dp_algorithm.m* is called by *dp.m* the name of the problem is composed out of the start/end points and the results directory is created. In the following lines all the discretization relevant variables are set.

2. The function *ndgrid* creates more dimensional matrices which allow to carry out a operation for all combinations of the operands at the same time. It enables also to use the same functions independent of the discretization. The inputs arguments of *ndgrid* contain the discretization of all dimensions (states and inputs). Resulting is for each dimension a variable which holds the discretization of this dimension in a sort of grid, that creates all combinations of the discrete points in the operation with the other dimension variables.

3. All external disturbances are grouped in one matrix *w*.

4. To avoid problems at the future interpolation a replacement of infinity is created here. It is called 'Big' and is chosen in such a way as to be higher than the highest possible cost. In the further text called *Big*.

5. The hard constraints are set (see Table 5.3.1.1)

6. If the result of an LP should be integrated, the resulting two control signals from the LP are loaded (CHP & electric Heating). Finally all parameters are saved to the results path.

Optimization Loop

1. Before the reverse time loop starts two other variables are set. *J_to_go* is the matrix where the cost-to-go during the optimization is stored in. All combinations which violate the final state constraint are directly set to *Big*. This final state constraint will normally not be touched by the final state values because the costs are interpolated between the discretization points and like this the final state constraint border is pushed up. This fact was respected when the final state values were chosen.

2. During the for-loop the system dynamics are analyzed, the constraints are checked and the costs are determined.

3. If the problem would be solved in succession to the solving of the LP for the electric cycle, some signal discretizations are replaced by the result of the LP. This is the case for the control signals of the CHP and the electric heating. In the case of the CHP the zeros (CHP 'off') are replaced. For the electric heating the control signal resulting from the LP is the only option, because the DP has normally no possibility to turn the electric heating on.

4. In every loop step the *lodge_heat_out* struct is reinitialized at 0.5 for state and *Big* for the cost elements. *Cost* is set to *Big* because afterwards all feasible cost values are replaced.

5. All combinations are evaluated in the *ndgrid_moro_model.m* function. This evaluation is done for one time step, here one hour. In the first loop step this means the system is developing from step $N-1$ to N. In this model function the equations of the Sections 4.2.1 and 4.2.2 are implemented. Additionally the model function generates costs depending on the state levels. These costs are explained in Table 5.3.1.1. All soft constraints, the CHP penalty and the heating hard constraint are at the end of the *ndgrid_moro_model.m* file. All the others are in the *dp_algorithm.m* file, at the lines following the function call of *ndgrid_moro_model.m*.

6. The *J_to_go* from the last loop step is replaced by one that is interpolated for the states at the end point of the model evaluation (*lodge_heat_out.x**) at this step.

7. Before the lowest costs are searched, those resulting of the model evaluation are added to the *J_to_go*.

8. Finally the optimal control signals for the starting point at this loop step are determined by the minimal costs and these are assigned to *J_to_go* for the next loop step. This is where the loop restarts.

After the loop all the results are saved to the */Results/'Problem Name'* folder.

Name	Description
Building soft constraint	The deviation of the building temperature from a comfort temperature ($17°C$) is weighted inversely proportional. If all soft constraints are fully violated over the whole time period, the total costs which arise are lower than turning on the CHP once. This is assured by dividing all soft constraints by the term *(numberofsoftconstraint · (N+1))*
WDWS (HTS, LTS) soft constraint	Similar to the building soft constraint, but the comfort temperature is $40°C$ for all tanks.
CHP penalty	When the CHP is turned on a penalty of 2 arises
Heating hard constraint	To turn on the heating system the LTS has to be above $35°C$, a violation of this constraint adds *Big* to the cost.
HTS/LTS hard constraint	The HTS temperature has to be above the LTS temperature to satisfy the layering assumption. Violation cost is *Big*.
Limit hard constraint	As soon as a state exceeds the lower discretization limit 0 *Big* arises as cost. To simplify the cost structure all heat tanks do saturate at their upper limit. This implicit constraint can be easily justified for the building and the LTS, where at the upper limit the warden would be requested to open the windows of the sleeping rooms respectively the warm water surplus can be brought to the fresh water supply tanks, where the energy storage amount is almost infinite. For the HTS and the WDWS this assumption violates in reality some physical constraints, because they do not have a physical connection to the fresh water supply. But as this saturation is only relevant in the case of an energy surplus it is not relevant for the optimality of the solution even though it has to be taken into account for further development of the heat tanks model.

Table 5.3.1.1: Cost structure

5.3.2 Forward Evaluation

1. All results and parameters of the optimization are loaded into the workspace.
2. An output struct is initialized (*out.**). To this struct the initial conditions entered by the function call from *dp.m* are assigned. For debugging and other purposes the cost development during the forward evaluation is stored too. Also some relevant variables for the autarky determination are initialized.
3. The forward time loop starts. At every step all the control signals are interpolated from the final state of the last time step. After the interpolation the control signals are rounded to the discrete values $(0, 1)$ due to rounding errors and equation validity. (See Equation 4.9)
4. Like in the backward optimization the control signals for the CHP and the electric heating are replaced, but the CHP signal is only replaced if the LP signal is bigger then the signal determined by the interpolation.
5. The model function is evaluated, the costs are calculated and the loop restarts with the next time step.
6. The results are saved for further processing, e. g., plotting.

5.4 Heuristic Controller

The heuristic controller (HC) is a combination of hysteresis and threshold switches. The switch-points are determined either based on information from the manufacturer or empirically. Some ideas to set switch-points were *copied* from the optimized solutions to improve the benchmark which the optimized problems are compared to. Those are especially the lower switch-point of the heating system and the consequent discharge of the LTS to leave room for new solar energy.

Supplier	**Demander**	**Supplier enabled**	**Supplier disabled**	**Constraints/ Remarks**
CHP	LTS	$25°C$	$30°C$	
CHP	HTS	$30°C$	$35°C$	
CHP	Battery	50% SOC	60% SOC	
Battery	HTS	98% SOC	95% SOC	Energy dissipation
Battery	LTS	$27°C$	$30°C$	$E_{SOC} \geq 60\%$
Battery	HTS	$32°C$	$35°C$	$E_{SOC} \geq 60\%$
HTS	WDWS	$35°C$	$45°C$	$T_{HTS} \geq 40°C \geq T_{WDWS}$
Battery	WWTP	100% WWTP-SOC	0% WWTP-SOC	
HS	Building	$10°C$	$12°C$	
HS	Building	$T_{LTS} > 50°C$	$T_{LTS} < 30°C$	

Table 5.4.0.1: Settings of the heuristic controller

The settings for the solar energy distribution are listed in Table 5.4.0.2. The goal was to represent the heuristically system behavior realistic with the TSC model. With the following quite simple rule, an acceptable system behavior resulted: The incoming energy is split between all active receivers. A receiver is active, if the associated constraints are fulfilled.

Receiver	**Constraints/ Remarks**
LTS	$T_{LTS} \leq 50°C$ and $T_{LTS} \leq T_{HTS}$
HTS	$T_{HTS} \leq 70°C$
WDWS	$T_{LTS} \geq 35°C$ and $T_{HTS} \geq 40°C$ and $T_{WDWS} \leq 70°C$

Table 5.4.0.2: Solar energy distribution by the heuristic controller.

In the model for the heuristic controller the same saturations for the warm water tanks were introduced. This was necessary to make a comparison to the optimized solution possible. Details about the saturations are listed in Table 5.3.1.1.

Chapter 6

Results and Discussion

Because the optimization process over the whole lodge service period leads even in the 64-bit MATLAB® to memory allocation problems, simulations where made for shorter periods of about three weeks. In the following section the results of three example time periods are discussed. These periods are:

1. **March:** 01.03.2006 - 31.03.2006
2. **April/May:** 22.04.2006 - 14.05.2006
3. **September:** 01.09.2006 - 20.09.2006

6.1 Grade of Autarky

Definition: *Autarky; adj. autarkic, self-sufficient; needing no help from others [7]*

As this definition is used mostly in an economic sense, it is freely adapted for physical systems as: A system's needs are met by the resources produced inside it and therefore no transactions across the system boarders are necessary. In this sense the sun is included in the system of the New Monte Rosa Lodge. The Grade of Autarky is a ratio to signify the self-sufficiency of the system. It maps the most important information provided by a simulation into a single number between 0% and 100%. This makes it easy to compare the performance of different controller behaviors.
The HA of the New Monte Rose Lodge is chosen such that it is able to reach a Grade of Autarky of at least 90% over a year period, whereas the non-electric energy for cooking is excluded [16]. This means that the energy supplied to the electric and the thermal cycle should be provided at least 90% from the PV cells and thermal solar collectors and at most by 10% from the CHP.

6.1.1 Grade of Autarky

The Grade of Autarky *goa* is defined as follows:

$$goa = \left(1 - \frac{E_{CHP} + Q_{CHP}}{E_{loss} + Q_{loss}}\right) \cdot 100 \quad [\%] \tag{6.1}$$

$$goa_{electric} = \left(1 - \frac{E_{CHP}}{E_{loss}}\right) \cdot 100 \quad [\%] \tag{6.2}$$

$$goa_{thermal} = \left(1 - \frac{Q_{CHP}}{Q_{loss}}\right) \cdot 100 \quad [\%] \tag{6.3}$$

E_{CHP}	Electric energy provided by the CHP
Q_{CHP}	Thermal energy provided by the CHP
E_{loss}	Total electric losses
Q_{loss}	Total thermal losses

If the *goa* is close to 100%, almost all power used is supplied by the PV or thermal solar collectors. A low *goa* denotes an high percentage of power supplied by the CHP.
The LP and DP algorithms are constrained such that the integrators have equal start and end values. However, the HC cannot be constrained in such a way, which leads to some impreciseness when calculating the autarky of the HC solution.

6.1.2 Autarky Overview

The following table gives an overview over the achieved grade of autarky in each simulated period.

The optimized controller is completely autarkic either in the electric or in the

Period	**electric**	**thermal**	**overall**	
	Optimized	Optimized	HC	Optimized
March	100.0%	93.0%	86.4%	93.0%
April / May	100.0%	100.0%	94.6%	100.0%
September	95.9%	100.0%	94.2%	95.9%

Table 6.1.2.1: Autarky overview

thermal subsystem in each simulated period. Therefore the overall autarky of the optimized controller can be calculated with the values listed in Table 6.1.2.2 and Equation 6.1, where

$$E_{CHP} + Q_{CHP} \quad = \quad t_{CHP} \cdot 3600\frac{s}{h} \cdot (P_{CHP,opt} + \dot{Q}_{CHP,opt}) \tag{6.4}$$

$t_{CHP} \cdot 3600\frac{s}{h}$	[s] Total seconds of CHP operation in the non-autarkic subsystem;
$P_{CHP,opt} = 14000$	[W] Produced electric power by the CHP in the operation point with the highest electric efficiency;
$\dot{Q}_{CHP,opt} = 27000$	[W] Produced heat by the CHP in the operation point with the highest electric efficiency.

This calculation implies that the autarkic subsystem receives additional energy from the CHP. The assumption does not influence the *goa*, however.

	$E_{CHP}[GJ]$	$Q_{CHP}[GJ]$	$t_{CHP}[h]$	$E_{loss}[GJ]$	$Q_{loss}[GJ]$
March	0	1.75	8	4.43	25.0
April / May	0	0	0	3.72	18.2
September	0.13	0	2.5	3.08	12.3

Table 6.1.2.2: CHP energy and total energy consumed by the HA and the lodge.

6.2 Discussion of the LP-optimized Battery-WWTP Subsystem

6.2.1 Expected Results

First of all the goal is to sensitize the reader to the information a result plot contains. For this reason, an easy virtual case is discussed. On the basis of Figure 6.2.1.1 it is easy to explain, what kind of results have to be expected. The upper graph shows the state of charge of the battery and the WWTP over time. During the weekend a lot of people are in the lodge, even if the weather is moderate only. Hence, the electric power consumption and the waste water production are high. On weekdays, there are only few people in the lodge. This is why almost no energy is consumed and no waste water is produced. The red line shows the behavior of a heuristic controller, the green line represents how a MPC manages the same situation. The lower graph shows on which days CHP action is necessary.
So let us have a look on this particular situation: After a weekend with a lot of vis-

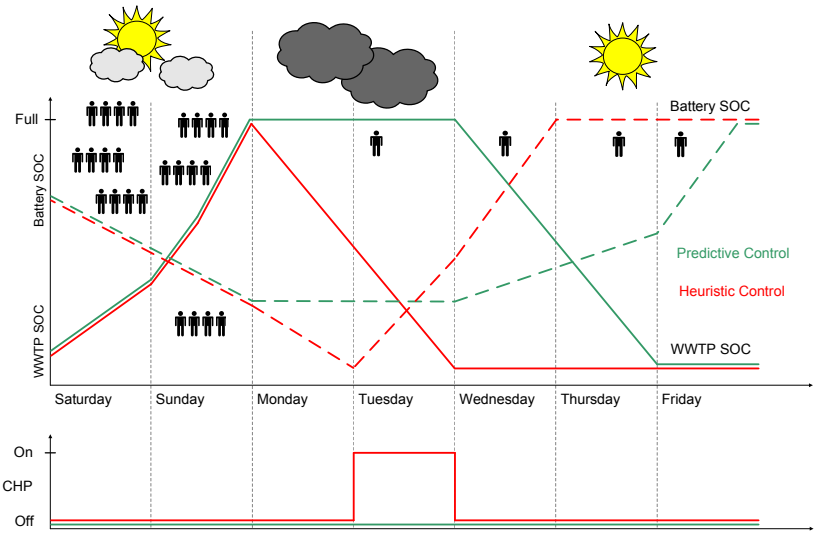

Figure 6.2.1.1: Qualitative representation of the expected results.

itors and moderate weather the energy budget of the system is at a marginal point. In this situation the heuristic controller would behave "conservative", because it simply follows certain algorithms, which are programmed the way some important constraints are never violated, even if the worst possible case would arrive. This means for this case, that it starts treating the waste water on Monday, which consumes a lot of electric power. This entails the activation of the CHP on Tuesday to charge the almost empty battery.
The MPC would handle the same time period differently. It has information about the future weather and booking schedule and has knowledge on the system behavior. Thus it *knows*, that only few visitors will come the next days and the waste water tank SOC will stagnate. That is why it does not treat the waste water until the bad weather period is over.
On Wednesday finally the weather is good again. Now there is sufficient energy to treat the waste water and fill the battery, so the system can start into the weekend with a full battery and an empty waste water tank. Unfortunately the heuristic

controller cannot profit as well as the MPC from the good weather period starting on Wednesday, because the battery has already been charged with the CHP on Tuesday. All solar energy won on Thursday and Friday must be dissipated, because the battery cannot store the whole amount.
This example illustrates the main advantages of MPC: It has information about the system behavior and future events and is able to include this additional information into the control algorithm. Because the MPC can drive the system to its boundaries, it can avoid ineffective power consumption.
An important remark: The question was never, if a model predictive controller with its outperforming but also computationally intensive technology is able to save energy *at all*, but *how much* it can save. That is why all simulations were made with an *ideal* MPC. With this setup, the performance bound of the present HA could be determined; a minimum necessary amount of fossil energy the HA consumes in order to fulfill the needs of the lodge.

6.2.2 Computed Results

In the following the results of the system optimization are presented; First a three week time period in September is discussed in detail. A second example is given in Section 6.2.4 where a time period in April/May is chosen to illustrate some further details. Finally the time period from the March 1^{st} to 31^{st} is discussed in Section 6.2.5.

6.2.3 September Period

Figure 6.2.3.2 shows the behavior of the system in the September period, when it is controlled with the optimal strategy computed by the LP, so that the performance bound is reached. Figure 6.2.3.1 shows the behavior of a simple heuristic controller.

Legend of Figures 6.2.3.1 and 6.2.3.2

Upper Subplot:

black:	$E_{SOC}[\%]$
red:	$P_{CHP}[100 \cdot W]$
cyan:	$P_{PV}[100 \cdot W]$
magenta:	$-P_{eH\_HTS}[100 \cdot W]$
green dotted:	$-P_{WWTP}[100 \cdot W]$
green dashed:	$-P_{stoch}[100 \cdot W]$
green solid:	$-P_{HA}[100 \cdot W]$
blue:	Sum of outgoing Powers $[100 \cdot W]$

Middle Subplot:

black:	$V_{WasteWaterPlant\_SOC}[\%]$
blue:	$\dot{V}_{WasteWater\_out}[10^{-6}m^3]$
cyan:	$\dot{V}_{WasteWater\_in}[10^{-6}m^3]$

Lower Subplot:

red:	$P_{CHP}[\%$ of $P_{CHP,max}]$

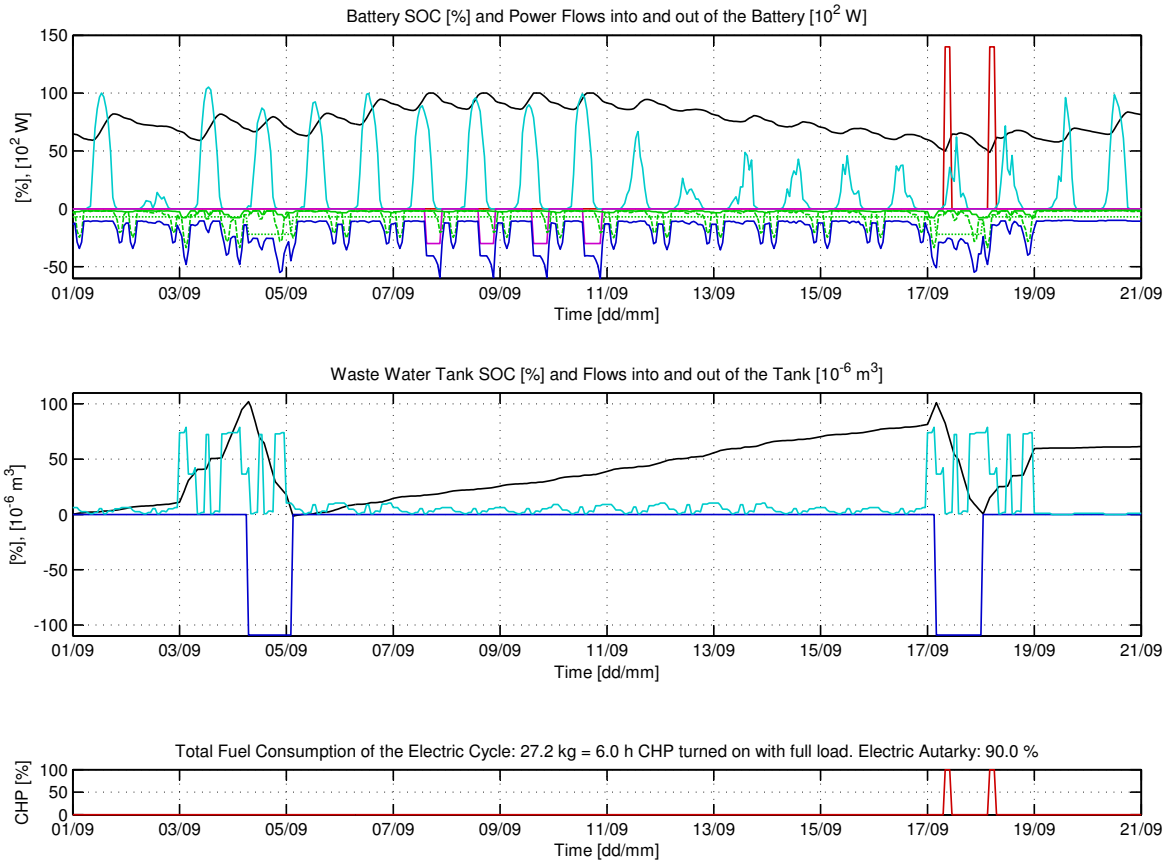

Figure 6.2.3.1: Battery and WWTP behavior in the time period from the September 1^{st} to the 20^{th} , when the system is heuristically controlled.

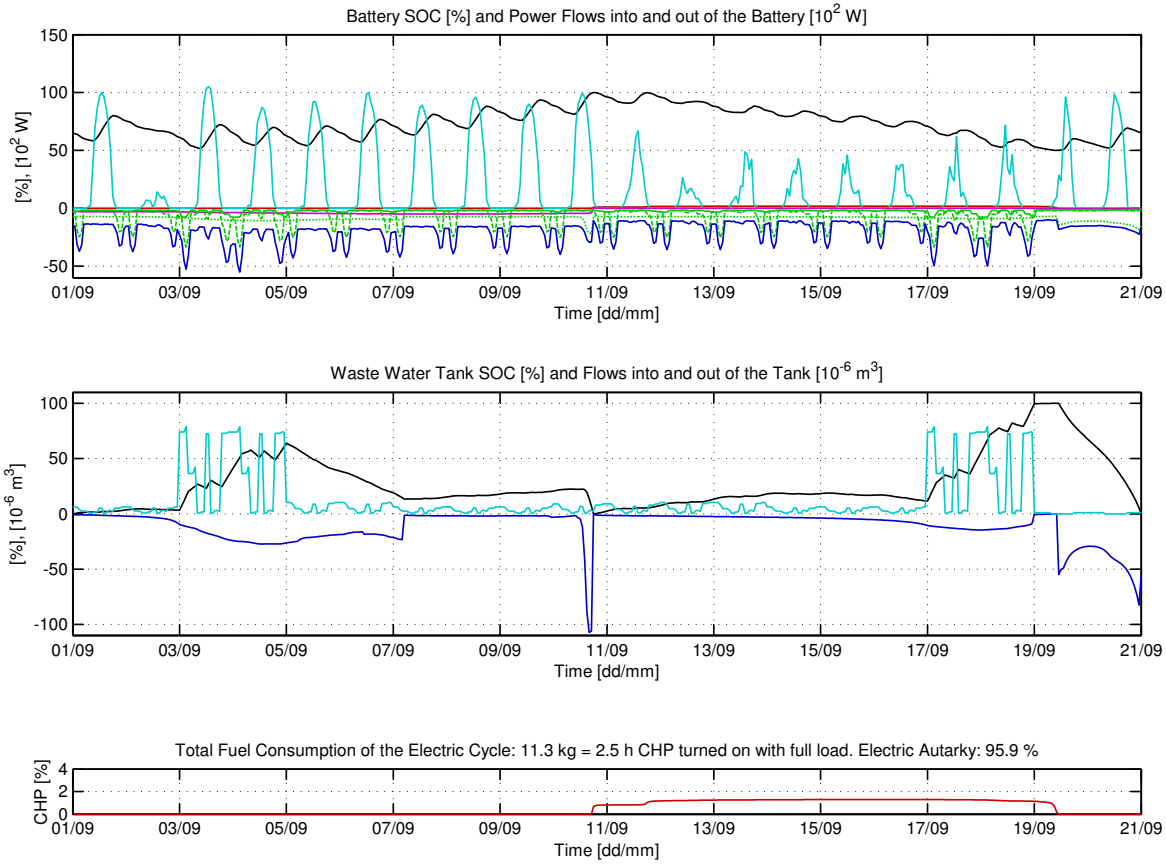

Figure 6.2.3.2: Optimized battery and WWTP behavior in the time period from the September 1^{st} to the 20^{th} .

Deterministic Inputs

The weather period and the number of visitors, which determine various system inputs, are equal for both controllers. These two inputs can be derived from the cyan curves. The weather is "proportional" to the cyan curve of the upper plot, e. g., a high power input into the battery implies sunny weather. The number of persons in the building is proportional to the waste water produced, which is represented by the cyan graph of the plot in the middle.
In the chosen time period the weather is rather bad. This is indicated by the produced peak power of the PV cells, which is approximately $5kW$ during 7 days. Besides that, the environmental temperature is around $0°C$ which can be seen in Figure 6.3.3.4. Furthermore, on two of three weekends the lodge is fully booked, i. e., 120 persons stay overnight. Bad weather combined with a high occupancy rate is very demanding for the system and therefore causes a higher CHP demand than a "regular" period. Nevertheless such a period is more interesting to discuss.
The blue curve in the upper plot indicates the energy leaving the battery. This amount of energy is determined only partly by the controller: The disturbance inputs influence the electric power consumption. Out of all energy flows leaving the battery only ctr_{eH_HTS} and ctr_{WWTP} can be controlled. (All power in- and outflows of the battery are described in Section 4.2.3.)
The blue curve in the middle plot describes the amount of waste water treated by the WWTP, which is proportional to ctr_{WWTP}.
Besides these signals also ctr_{CHP} is set by the controller. The red curve in the upper plot indicates the power supplied by the CHP.

How to Interpret the Results

Before analyzing the behavior of the optimized controller and comparing it to the heuristic one, a short side note is given on the computed output of the controllers (e. g., ctr_{CHP}): The heuristic controller consists of threshold switches, which always give either 0 or 1 as output. Unlike the output calculated by the LP, it takes arbitrary values between 0 and 1 although in reality the CHP will only be turned on with full load to reach the maximum efficiency (i. e., like the resulting output of the HC). However, this is not a problem for the interpretation of the results provided by the LP. A short example is given to illustrate this: The optimal solution asks for turning the CHP on with 25% load during one hour. This is equivalent to turning the CHP on with full load for 15 minutes. The same principal is effectual for ctr_{WWTP} and ctr_{eH_HTS}. To constrain the solution of the optimization problem to values of either 0 or 1 leads to a *mixed integer problem*. Such a system could be modeled with *Hysdel*, the hybrid system description language developed by the Automatic Control Laboratory of ETH Zurich. (Check http://control.ee.ethz.ch/∼hybrid/hysdel/). In general, these problems are computationally more intensive.

Configuration of the HC

The heuristic controller is configured as follows: It empties the waste water tank completely, when it reaches its maximum level. It starts the CHP to generate electric power, if the battery SOC is under 50%. It enables electric heating, when the battery SOC reaches 98% and disables it at 95%. It also activates electric heating and the CHP, if elements of the heating cycle fulfill certain constraints. (For further details see Section5.4.) Therefore one must pay attention to the *point of time* the CHP is activated. From that one can conclude, if the CHP is activated due to a demand of energy from the electric or the thermal cycle.

CHP and Electric Heating Handling of the HC

Over the time period of three weeks, the CHP is activated for 6 hours and consumes $27.2kg$ of fuel which leads to a partial autarky of the electric cycle of $goa_{electric} = 90\%$. The CHP supplies the electric cycle with overall $6h \cdot 14kW = 84kWh$. In the same period electric heating is activated for 29 hours due to excess of electric energy in the battery. This is equivalent to $29h \cdot 3kW = 87kWh$ electric energy, i. e., more than supplied by the CHP. Although more energy is dissipated due to excess than demanded by the CHP, it cannot be concluded that their exists a better controller strategy, which necessarily can avoid CHP usage. This is because the size of the battery has to be considered, which limits the amount of energy that can be shifted in time.

Waste Water Treatment Handling of the HC

The blue curve of the middle plot shows, that the waste water is treated at the same time as the lodge is fully booked, which is not a desirable situation. During these weekends the electric power demand is high anyway due to the large number of visitors, therefore the waste water tank should ideally not be emptied at that point of time. On September 3^{rd} and 4^{th} , the treatment does not have any negative consequences due to the good weather, which allows the battery to recharge during the day. However, on the weekend of the 17^{th} the incoming solar power added up with the energy stored in the battery is not sufficient to meet the entire electric power demand. As a consequence the battery reaches its lower SOC bound and the CHP must be turned on.

Configuration of the Optimized Controller

The problem is set up, such that the total fuel consumption is minimized. The final state of the system is constrained to be equal to the initial state. The initial state can be chosen arbitrarily. Of course all constraints must be satisfied.

CHP and Electric Heating Handling of the Optimized Controller

Actually, only three out of four possible combinations of the input signals ctr_{CHP} and ctr_{eH_HTS} occur over time: $ctr_{CHP} = 0$ and $ctr_{eH\_HTS} > 0$, $ctr_{CHP} > 0$ and $ctr_{eH\_HTS} = 0$, or $ctr_{CHP} = 0$ and $ctr_{eH\_HTS} = 0$. Both control inputs set to a positive value at the same point in time is never an optimal solution. Thus, one can assign each time period to one of these three modes:

1. Mode 1: $ctr_{CHP} = 0$ and $ctr_{eH\_HTS} > 0$: The system dissipates energy due to excess of electric power provided by the PV. Here, this can be seen in the time period from September 1^{st} to 10^{th} .

2. Mode 2: $ctr_{CHP} > 0$ and $ctr_{eH\_HTS} = 0$: The system has insufficient power input, it needs additional energy from the CHP. The time period from September 10^{th} to 19^{th} can be assigned to this case.

3. Mode 3: $ctr_{CHP} = 0$ and $ctr_{eH\_HTS} = 0$: The system is balanced, no energy has to be dissipated or additionally supplied by the CHP. This case occurs from the September 19^{th} to 21^{st} .

When the system changes from Mode 1 to Mode 2, the battery is filled completely und the WWTP is empty. This is obvious, because otherwise the energy would not be dissipated during Mode 1 but instead stored in the battery or used to treat the waste water to avoid using energy from the CHP.

When the system changes from Mode 2 to Mode 1, the battery is empty and the WWTP completely filled. If this would not be the case, less energy could be provided by the CHP during Mode 2.

Interpretation of the Waste Water Tank as Inverse Battery

The wastewater tank is able to store up to $5.5m^3$ waste water. To treat this $1494W \cdot 14h \approx 75MJ$ is needed, which is approximately $\frac{1}{7}$ of the suitable energy stored in the battery. Actually, the following is true: The case where the WWTP is completely full and the energy to treat the contained waste water is stored in the battery is equivalent to the case where the WWTP is empty and the energy to treat the waste water is no more in the battery. Thus, one can interpret the waste water tank as an inverse battery. This idea is sketched in Figure 6.2.3.3.

Merge Waste Water Tank and Battery into a Single State Variable

From this sight can be concluded, that the WWTP and battery can be viewed together as one state. There is only one direction to move along namely normal to the equipotential lines. The constraints can easily be converted to rules for the merged state E_{tot}. A simple underlying controller can adopt, when exactly the WWTP should be activated. Treating the waste water is moving along an equipotential line, i. e., does not generate any cost in the optimization algorithm.
However, this fact is not explored in detail in this thesis, further analysis should

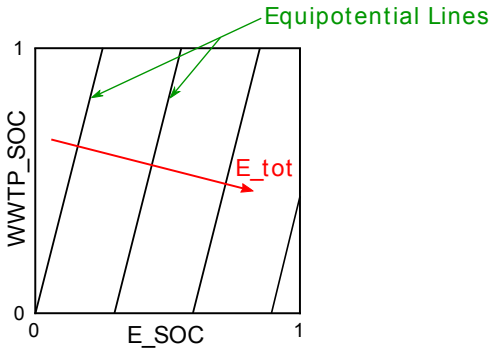

Figure 6.2.3.3: Draft of the new state variable "E_{tot}". Moving along the equipotential lines needs some time but does not induce cost to the system. The maximum value of E_{tot} is reached, when $E_{SOC} = 1$ and $WWTP_{SOC} = 0$. The minimum value is reached in the opposite case.

follow in order to prove what has been derived theoretically here.

6.2.4 April/May Period

Heuristic Control

This example illustrates very well, how bad a heuristic controller can drive the system compared to an optimized one. The upper graph of Figure 6.2.4.1 shows a very high CHP activity around May 1^{st} . Also one can see, that E_{SOC} never reaches the lower bound, which induces, that the CHP is always activated due to a demand of heat by the thermal cycle. From first sight one might guess, that there is plenty of energy in the system overall but badly distributed, i. e., changing the conditions in which electric heating is turned on solves the problem. However, this is not the case, as shown in Figure 6.2.4.3): Changing the switch-points on the electric heating even worsens the autarky because it immediately leads to a lack of electric

energy. It turns out, that the heuristic solution cannot be improved significantly, unless comfort is reduced dramatically.

Optimized Control

By treating the waste water constantly instead of dissipating energy into the HTS the optimized controller makes use of the large amount of electric energy produced by the PV cells at the beginning of the time period. Like this, the battery is fully charged on April 27^{th} and the tank is filled by 20%. The energy stored in battery and the almost empty tank are together sufficient to bridge the critical phase up to May 4^{th} . This is an acceptable behavior: The optimized controller does not use the CHP *at all* and still fulfills the constraints. Up to the April 25^{th} and from May 4^{th} to the end of the simulation the system is in Mode 1, while in the rest of the time the system is in Mode 3.

Legend of Figures 6.2.4.1, 6.2.4.2 and 6.2.4.3

Upper Subplot:

black:	$E_{SOC}[\%]$
red:	$P_{CHP}[100 \cdot W]$
cyan:	$P_{PV}[100 \cdot W]$
magenta:	$-P_{eH\_HTS}[100 \cdot W]$
green dotted:	$-P_{WWTP}[100 \cdot W]$
green dashed:	$-P_{stoch}[100 \cdot W]$
green solid:	$-P_{HA}[100 \cdot W]$
blue:	Sum of outgoing Powers $[100 \cdot W]$

Middle Subplot:

black:	$V_{WasteWaterPlant\_SOC}[\%]$
blue:	$\dot{V}_{WasteWater\_out}[10^{-6}m^3]$
cyan:	$\dot{V}_{WasteWater\_in}[10^{-6}m^3]$

Lower Subplot:

red:	$P_{CHP}[\%$ of $P_{CHP,max}]$

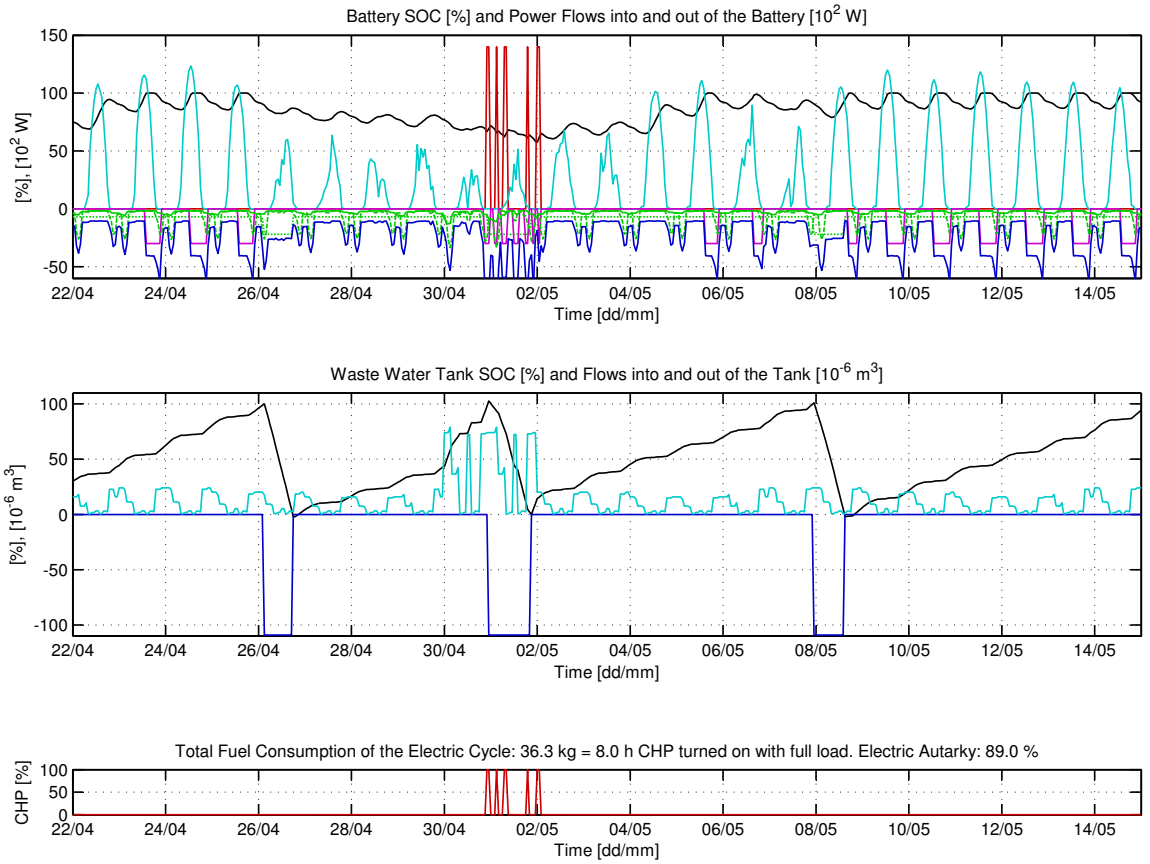

Figure 6.2.4.1: Battery and WWTP behavior in the time period from April 22^{nd} to May 14^{th} , when the system is heuristically controlled.

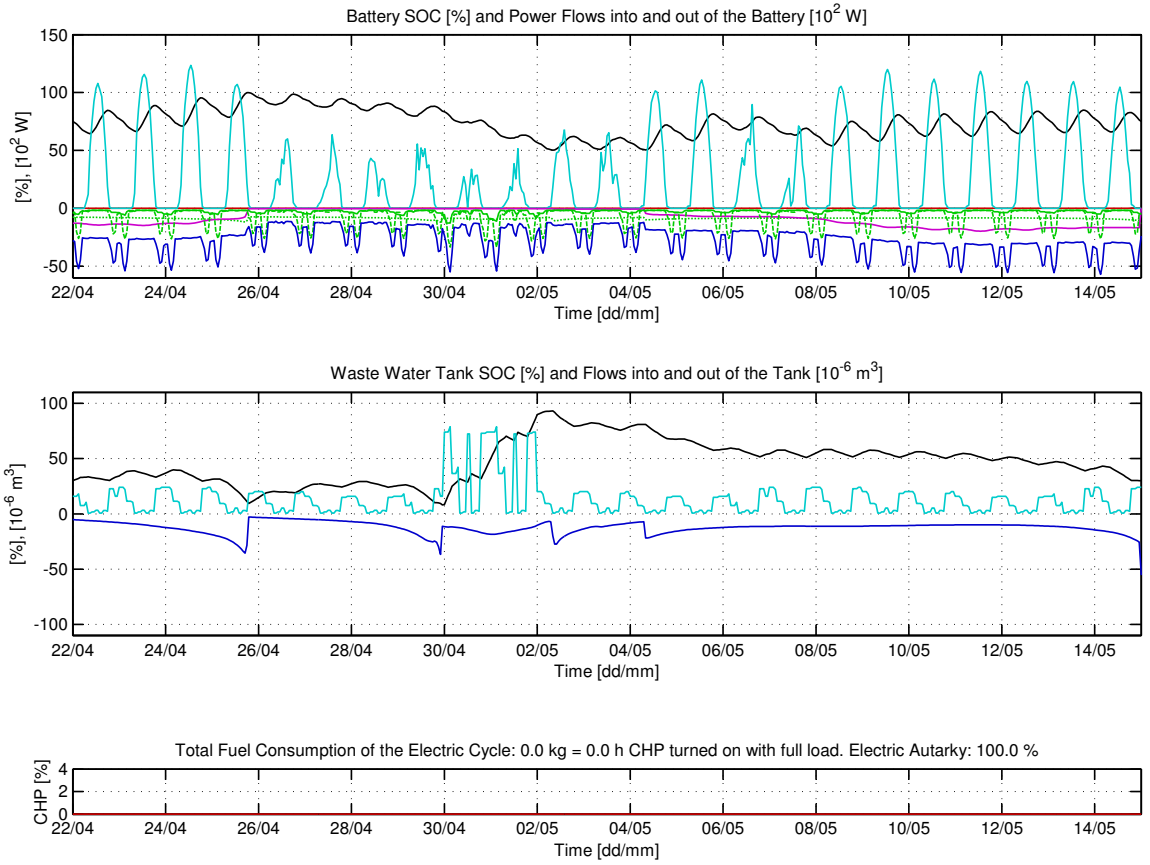

Figure 6.2.4.2: Optimized battery and WWTP behavior in the time period from April 22^{nd} to May 14^{th} .

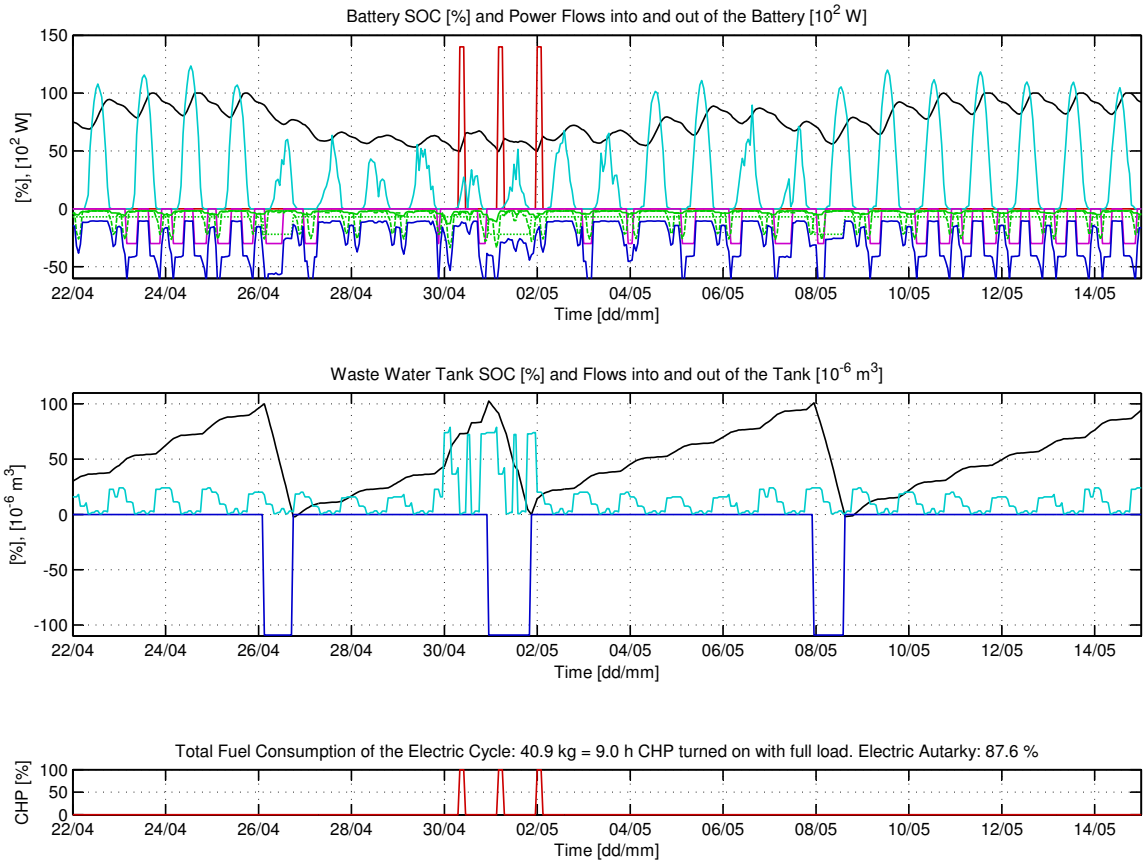

Figure 6.2.4.3: Battery and WWTP behavior in the time period from April 22^{nd} to May 14^{th} , when the system is heuristically controlled and the electric heating switch-points are augmented, such that altogether more energy is transferred from the electric to the thermal cycle.

6.2.5 March Period

In March the outside temperature is quite low and only few people visit the lodge. This implies, that electricity use and waste water production are reduced. The solution of the LP reflect this fact: the optimized solution demands no energy from the CHP for the electric cycle. In contrast the heuristic controller turns on the CHP for 27 hours. This is due to the fact, that even the optimized thermal cycle demands a huge amount of heat from the CHP, which can be seen in Figure 6.3.3.6.

Legend of Figures 6.2.5.1 and 6.2.5.2

Upper Subplot:

black:	$E_{SOC}[\%]$
red:	$P_{CHP}[100 \cdot W]$
cyan:	$P_{PV}[100 \cdot W]$
magenta:	$-P_{eH\_HTS}[100 \cdot W]$
green dotted:	$-P_{WWTP}[100 \cdot W]$
green dashed:	$-P_{stoch}[100 \cdot W]$
green solid:	$-P_{HA}[100 \cdot W]$
blue:	Sum of outgoing Powers $[100 \cdot W]$

Middle Subplot:

black:	$V_{WasteWaterPlant\_SOC}[\%]$
blue:	$\dot{V}_{WasteWater\_out}[10^{-6}m^3]$
cyan:	$\dot{V}_{WasteWater\_in}[10^{-6}m^3]$

Lower Subplot:

red:	$P_{CHP}[\%$ of $P_{CHP,max}]$

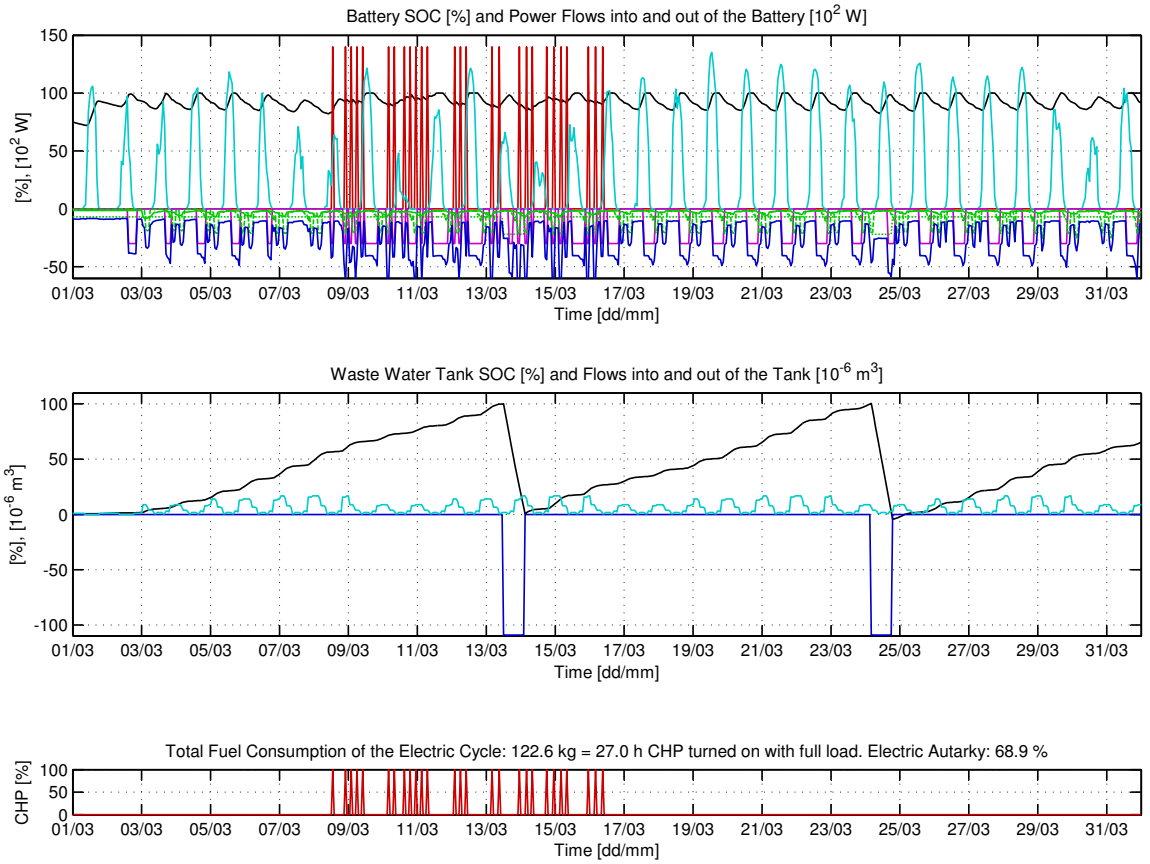

Figure 6.2.5.1: Battery and WWTP behavior in the time period from March 1^{st} to 31^{st} , when the system is heuristically controlled.

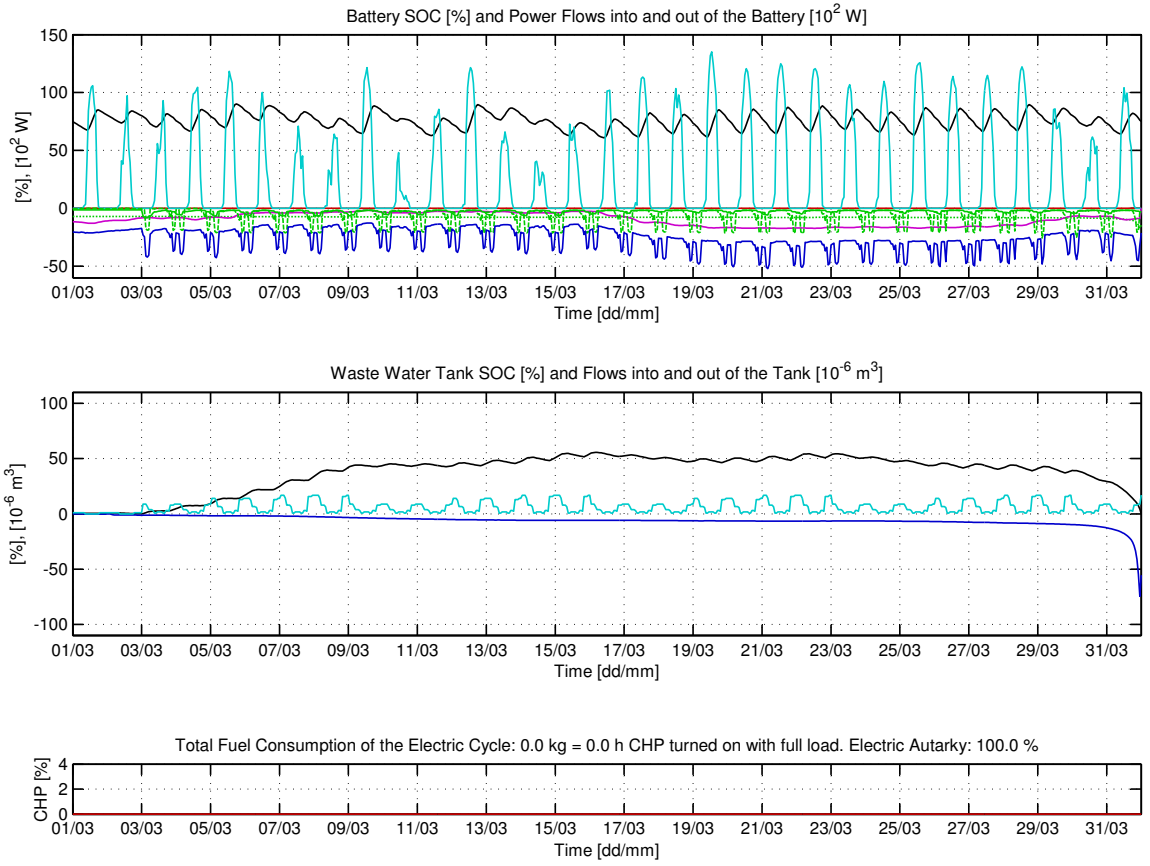

Figure 6.2.5.2: Optimized battery and WWTP behavior in the time period from March 1^{st} to 31^{st} .

6.3 Discussion of the DP-optimized Thermal Subsystem

The main advantage of the optimized controller is the heat management between the different warm water tanks. As explained below the final settings for the HC concerning the building temperature produce an almost as good behavior as the DP solution does.
It is to say that the HC was adapted after some simulations and comparisons with the optimized solutions from different time periods. In the final setting some switch-points are set very similar to the ones of the DP solution, e. g., the lower building temperature switch-point is set to $10°C$. This is the critical temperature where even the optimized controller turns on the CHP to support the heating, although this is a very rare case in the optimized solution. With these adaptations of the HC it is now possible to compare the solutions and the autarky of the two concepts. The $10°C$ boundary of the optimized solution is caused by interpolation errors which appear if the DP algorithm interpolates the hard constraint at $7°C$. Due to the interpolation the high cost level of the hard constraint is moved into the feasible area.
In the following sections three different periods are discussed. Only the important differences are outlined, but the general behavior of the two concepts is similar.
A difference between the results of the HC and the DP which could lead to misinterpretation is actually only an issue of configuration. The HC keeps control signals set *on* as long as the conditions are satisfied. This induces, e. g., in the case of ctr_{TSC_LTS}, that it is turned on also at night when no energy is available from the thermal solar collectors. Unlike the optimized solution: it turns on the separate signals only when energy is available. This difference does not affect the energy household, both concepts use the whole amount of available energy.

Special Case: Electric Heating

As the electric heating is part of both, thermal and electric, cycles it is only part of the heuristic solutions. In the optimized solution ctr_{elH_HTS} is set to 0 at all time. This leads to more available heat energy for the heuristic case what helps the HC to achieve a higher grade of autarky *goa*. In the Figures 6.3.3.1 to 6.3.3.6 the electric heating control signal is not visualized, but always when the HTS is heated without ctr_{CHP} or ctr_{TSC_HTS} turned on the electric heating is the energy source. This is mostly the case at the second half of sunny days, where the battery normally gets close to the upper limit.

6.3.1 April/May Period

This period is visualized in Figures 6.3.3.1 and 6.3.3.2.

Building Temperature

The building temperature behaves very similar in both concepts, except that it is constantly some degrees higher in the optimized solution. The optimized controller distributes the energy better between the tanks which improves the losses and the heat transitions.

CHP

On May 1^{st} the HC is urged to activate the CHP several times. After the switch-point of $10°C$ is hit the HC heats up the building to $12°C$. This causes a lot of ' unnecessary ' CHP action. The margin of $2°C$ is set to avoid oscillations of the CHP over a longer period. But in this case the CHP action is not unnecessary at all because the electric cycle demands exactly the same amount of CHP at almost the same time. This can be checked by setting the heating switch-point to a lower level (e. g., $7°C$), such that no CHP is needed from the thermal cycle.
During the same days the optimized controller uses also the little available solar energy to heat the building. Like this a temperature between 10 and $11°C$ is maintained until more solar energy is available and therefore no CHP support is needed by the optimized controller. This is a clear advantage of the predictive controller as it can estimate how much energy is needed to bridge the bad weather period.

Warm Water Tanks

In the optimized solution the WDWS is heated by the HTS. This interconnection is only barely used by the HC. This is because the WDWS is heated with solar energy in the HC solution although this energy would be needed to heat the building. In general the optimal solution keeps the temperature of the WDWS and the HTS closer to each other than the HC does. In general the optimized controller is able to provide more warm drinking water.
The HC suffers from the assumption about the HTS and LTS interconnection. A further example for this problem is discussed in Section 6.3.3 about the March period.

6.3.2 September Period

(See Figures 6.3.3.3 and 6.3.3.4)
Both, the optimized and the heuristic controller use the available solar energy at the beginning of the period to heat the building. With this big amount of energy stored in the building mass the bad weather period after September 11^{th} can be bridged easily. With both concepts the building temperature is always above $15°C$, what represents a very high comfort level.

CHP

With support of the CHP, which is caused by the electric cycle during the second weekend of this period, the HC has over all more energy available in the warm water tanks. One consequence is that it could provide a little bit more warm drinking water than the optimized controller. But as the temperature in both systems is always above $35°C$ the warm water supply is anyway guaranteed at all time. Obviously, the HC benefits also from the CHP energy to heat the building.

Heating System

As the HC controller stops heating as soon as the building temperature reaches the upper limit, the optimized controller realizes that this heating energy would be lost and stops heating by itself. It stops at that exact moment to provide enough storage room in the LTS to save all the available solar energy the next day, otherwise it uses the heating energy surplus above the saturation to compensate the losses.

This is possible since the difference equation is evaluated every hour and after the evaluation the saturation limits are applied.
The heating of the building is represented by the lilac signal row. In the September period the heating breaks occur during the lilac gaps on September 6^{th} and September 9^{th} .
The saturation was set because a temperature far above $20°C$ is not very comfortable for the sleeping rooms. In reality the saturation could stand for guests asking the warden to open the windows. For the DP solution first a cost at the upper limit was introduced to avoid the saturation problem. Unfortunately, this led to cost rounding errors so that the temperature of the building was decreased by several degrees. The saturation leads to a much nicer solution and has the same effect.

6.3.3 March Period

This period illustrates in the Figures 6.3.3.5 and 6.3.3.6 that the optimized controller needs the CHP in some cases. The outside temperature is very low in this period and the solar irradiation is not always that strong as it is in the high season. The HC consumes $123kg$ fuel and the optimized controller consumes $82kg$. It is to say that the HC takes also the electric cycle into account, which may cause a part of the fuel consumption. However, in this case the electric cycle does not need any CHP (see Figure 6.2.5.2). The performance of the HC is improved marginally by changing the switch-points of electric heating (like in the May example of the LP results, Section 6.2.4). With the additional electric heating the HC fuel consumption is about $118kg$.

CHP / Warm Water Tanks

From May 9^{th} to the 17^{th} the CHP is turned on by the HC and by the optimized controller. In the case the HC controls the system, the HTS is already at a high temperature at the beginning of the period and therefore hits the upper saturation limit very fast. The HTS dissipates energy and the CHP is turned on over and over again to heat the LTS. As discussed in Table 5.3.1.1 the saturation of the HTS in not physically realizable. Those are weak points of the warm water tank model. Among others the layering assumption of the tanks is challenged to be inaccurate or even wrong. The model could probably be improved by a parameter identification for the time constant (Equation 4.8), which determines the speed of the heat transfer from the HTS to the LTS. As the heating of the building only takes energy from the LTS, a distributed heating energy source, e. g., from HTS and LTS, could also help to solve this problem. But a validation of any improvement of the modeling of the heating tanks as well as for the whole model is not possible as long as the lodge is not built.
During the other periods this problem is less obvious as there is no repeated CHP action. For the optimized controller this is in general a smaller problem as it uses the interconnection to the WDWS to lower the HTS.

Legend of Figures 6.3.3.1, 6.3.3.2, 6.3.3.3, 6.3.3.4, 6.3.3.5 and 6.3.3.6

Upper Subplot:

blue:	$T_{WDWS}[°C]$
red:	$T_{HTS}[°C]$
green:	$T_{LTS}[°C]$

Middle Subplot:

blue:	$\dot{Q}_{WDWS}[10^3 W]$
red:	$\dot{Q}_{persons}[10^3 W]$
yellow:	$\dot{Q}_{Solar}[2.8 \cdot 10^3 W]$
magenta:	$T_B[°C]$
dark green:	$T_{env}[°C]$

Lower Subplot:

black:	$ctr_{CHP}[-]$
lila:	$ctr_{HS}[-]$
magenta:	$ctr_{WDWS\_HTS}[-]$
blue:	$ctr_{TSC\_WDWS}[-]$
red:	$ctr_{TSC\_HTS}[-]$
green:	$ctr_{TSC\_LTS}[-]$

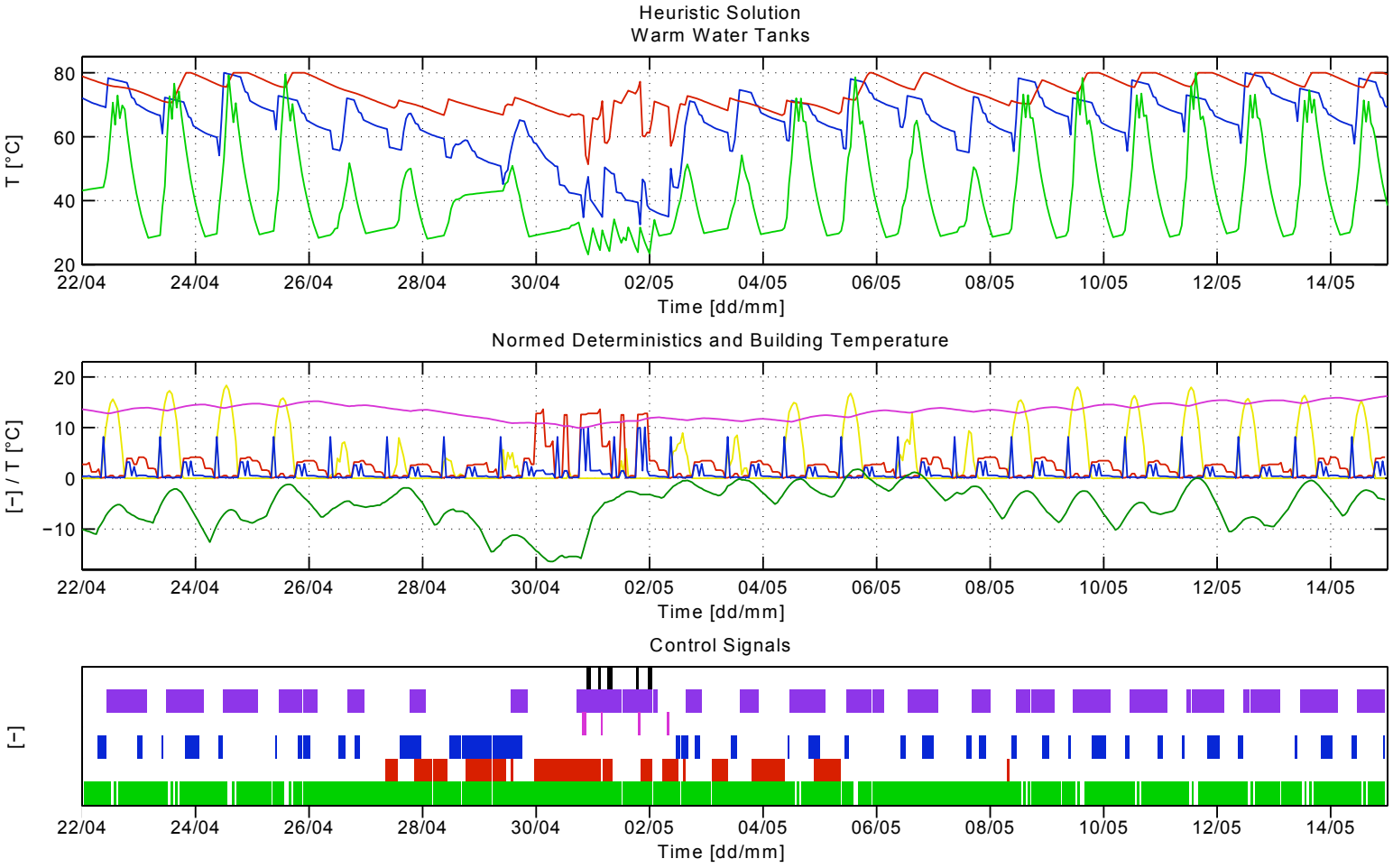

Figure 6.3.3.1: Thermal cycle behavior in the time period from April 22^{nd} to May 14^{th}, when the system is heuristically controlled.

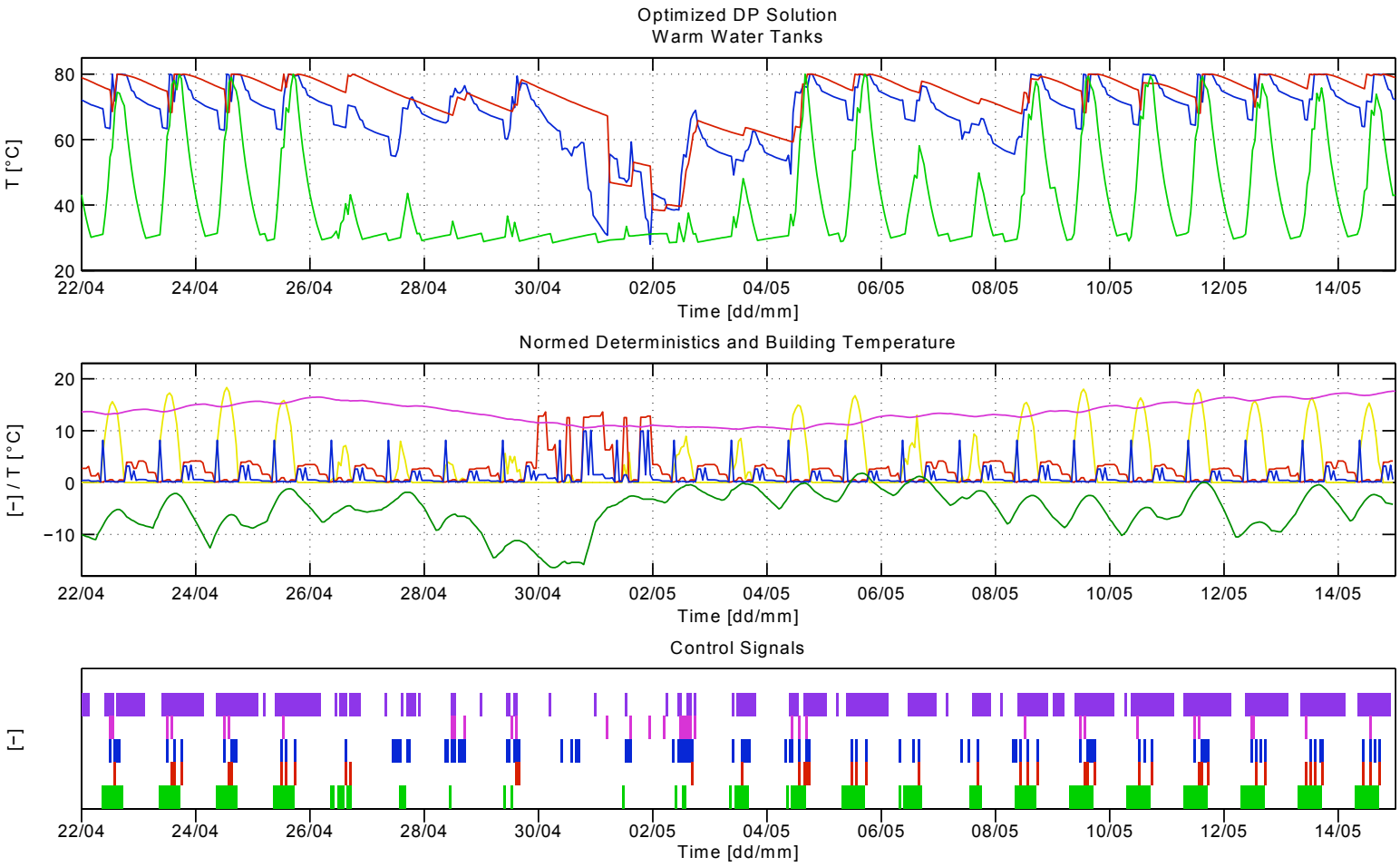

Figure 6.3.3.2: Optimized behavior of the thermal cycle in the time period from April 22^{nd} to May 14^{th}.

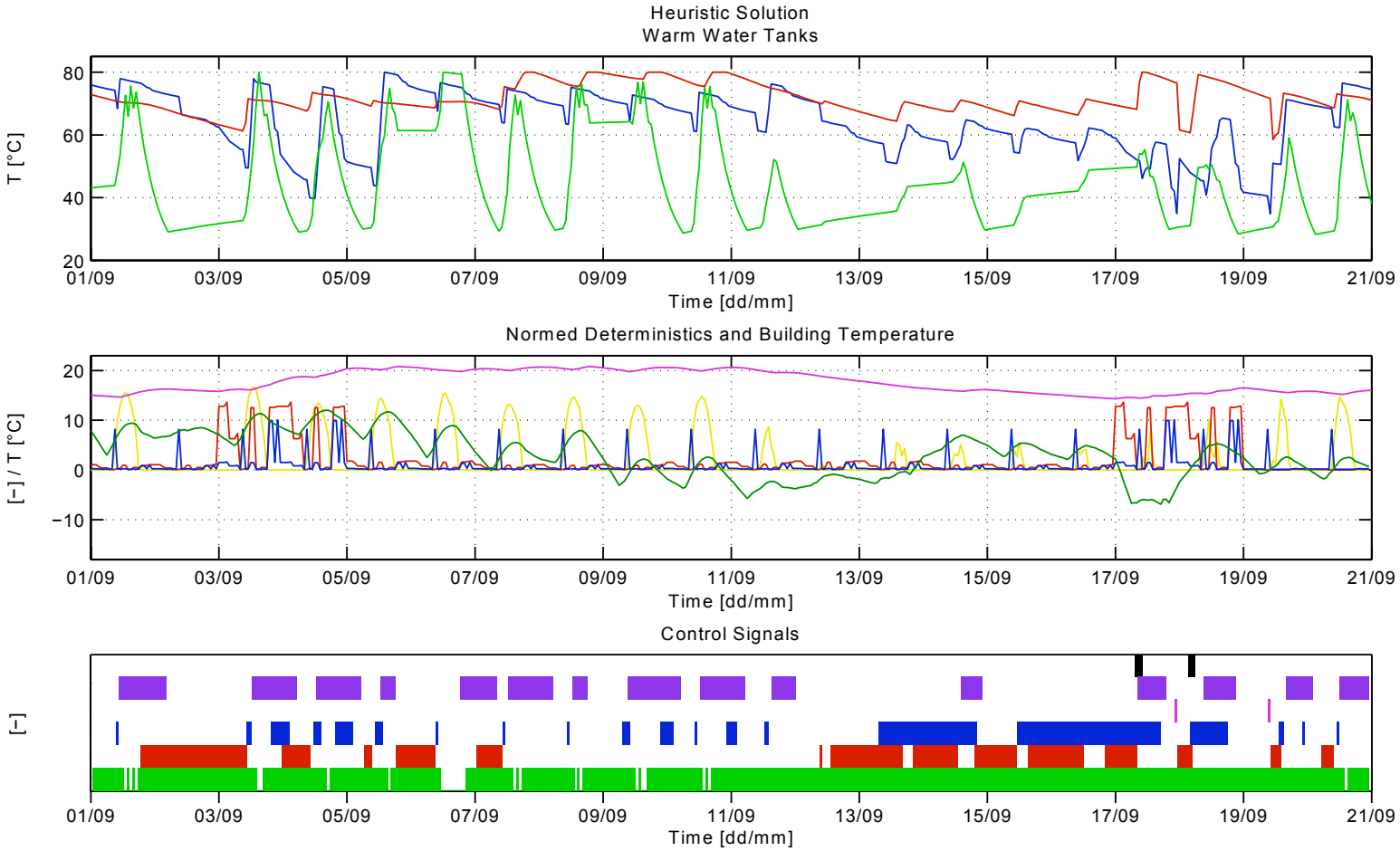

Figure 6.3.3.3: Thermal cycle behavior in the time period from September 1^{st} to September 20^{th}, when the system is heuristically controlled.

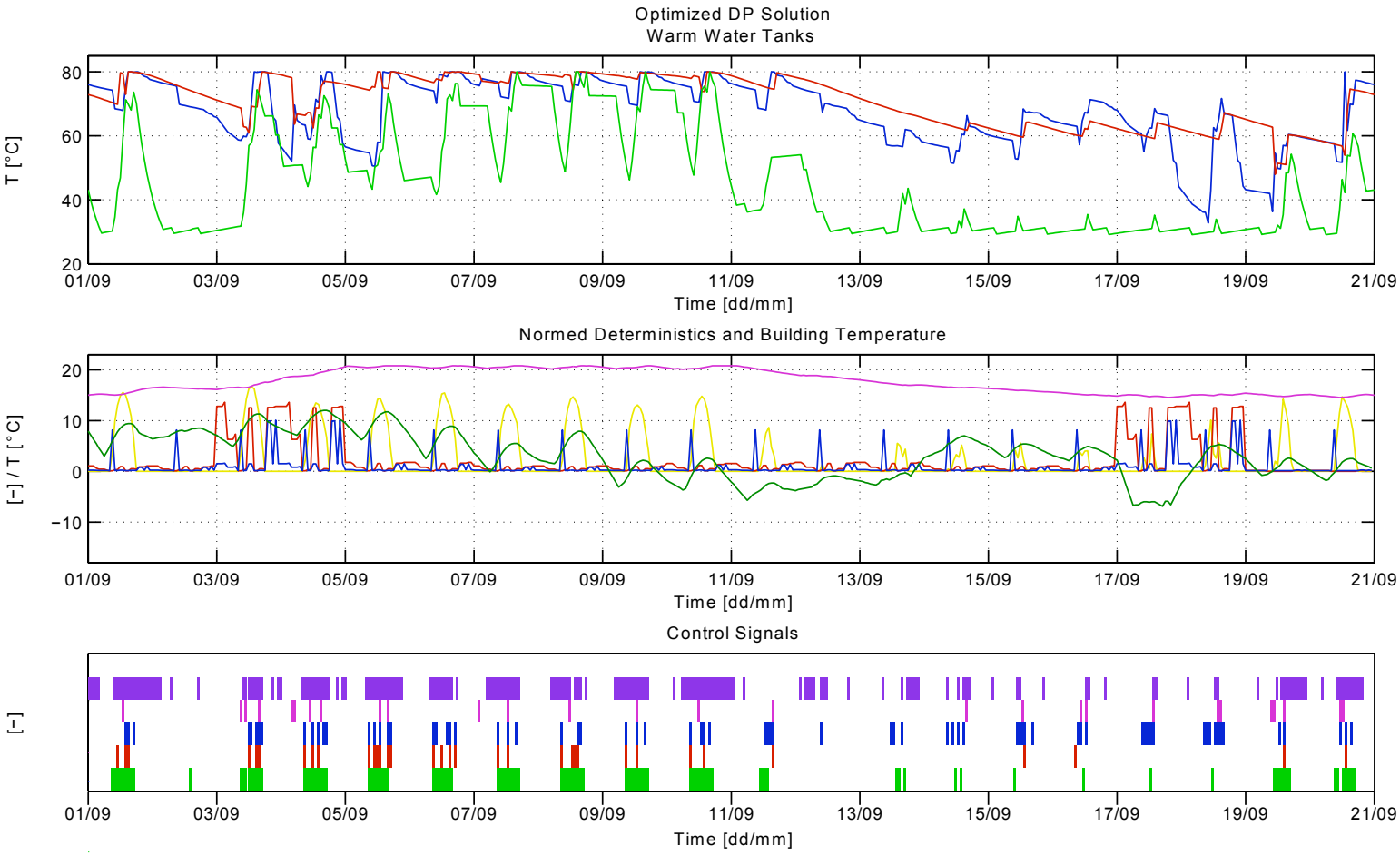

Figure 6.3.3.4: Optimized behavior of the thermal cycle in the time period from September 1^{st} to September 20^{th}.

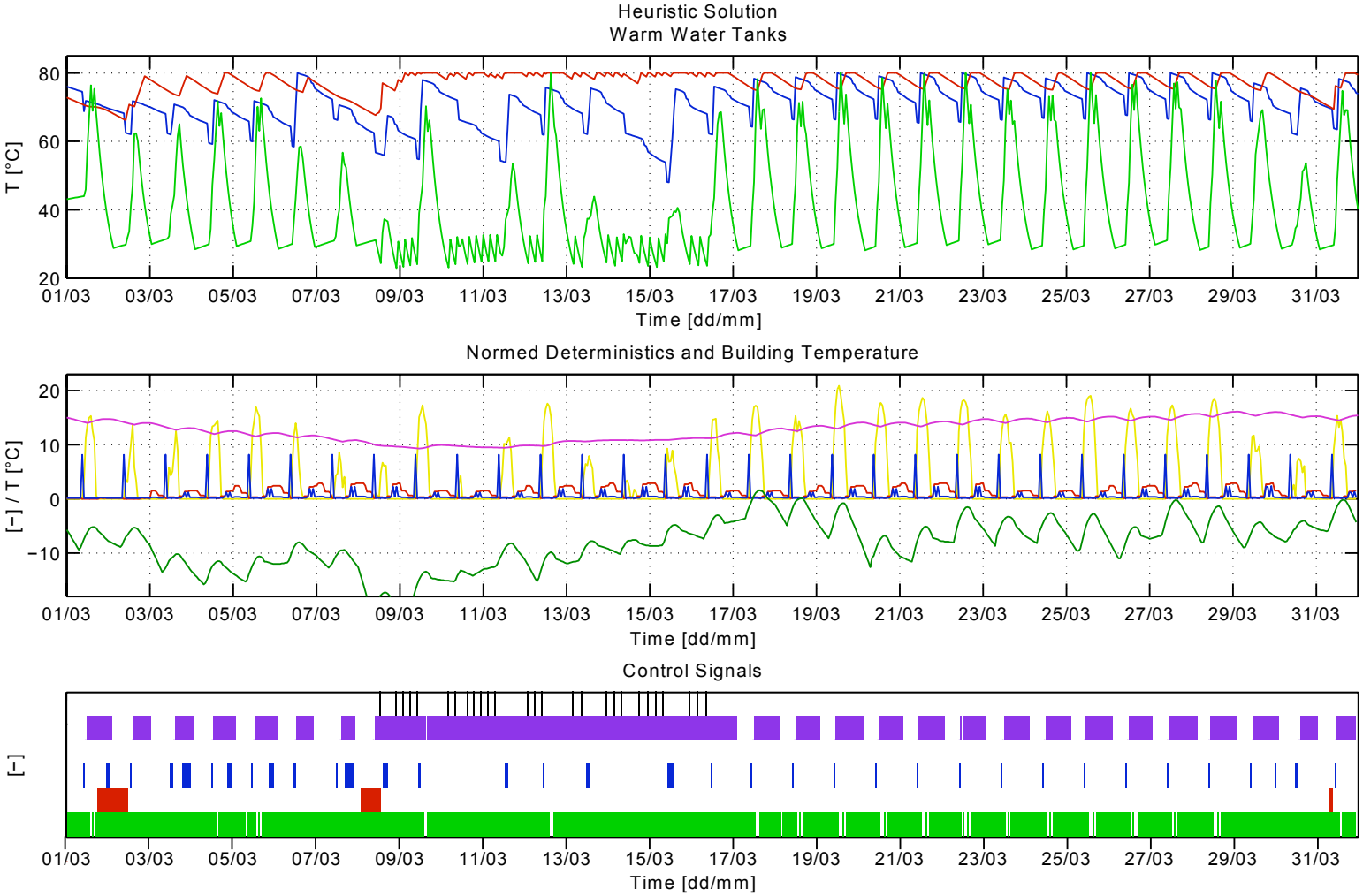

Figure 6.3.3.5: Thermal cycle behavior in the time period from March 1^{st} to March 31^{th}, when the system is heuristically controlled.

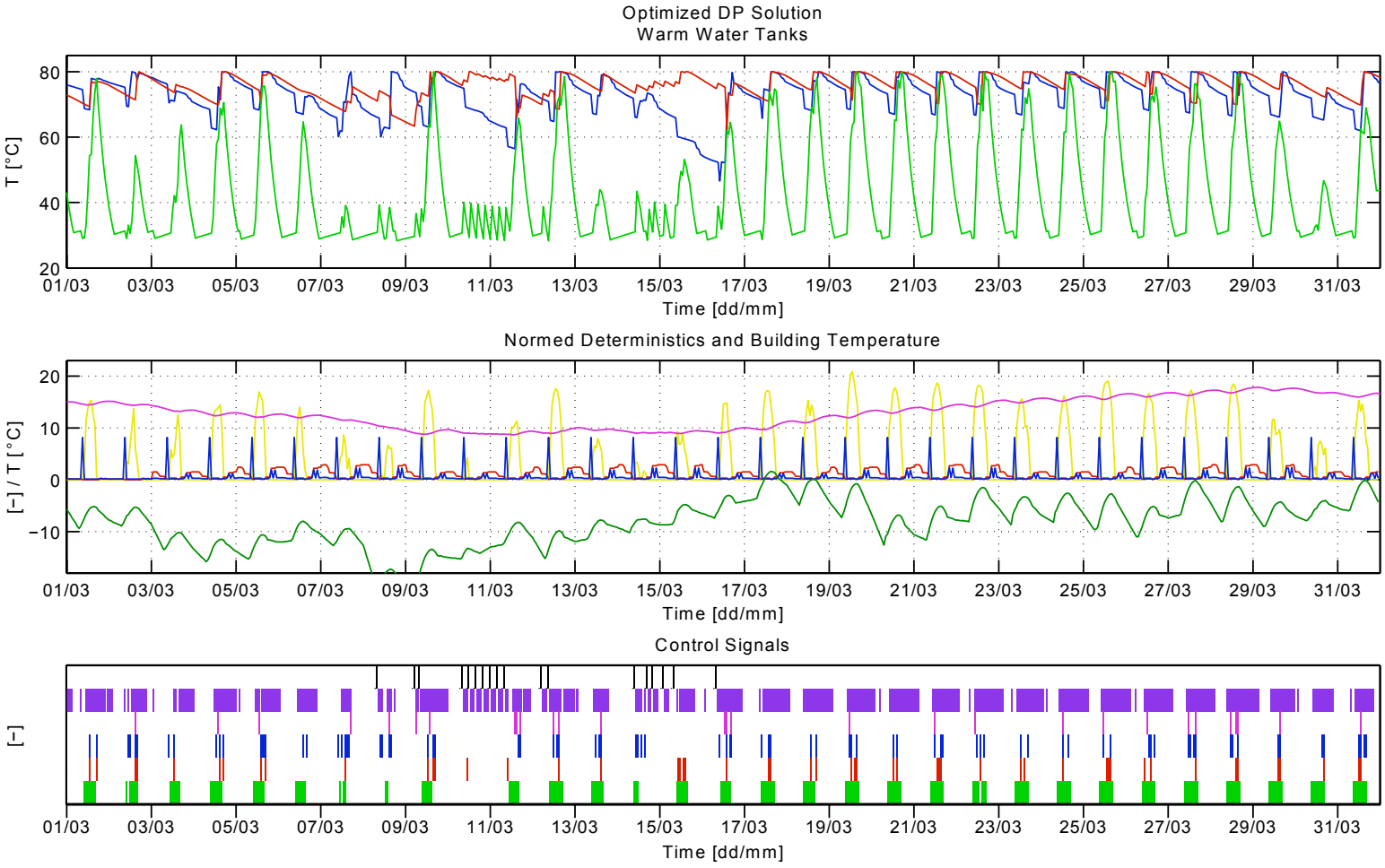

Figure 6.3.3.6: Optimized behavior thermal cycle in the time period from the March 1^{st} to March 31^{th}.

6.4 Conclusions and Future Prospect

6.4.1 Some General Facts Explored

Energy shortages for the thermal or the electric subsystem occur always at similar situations: From the simulation one can clearly see, that the thermal subsystem suffers a lack of energy when the outside temperature T_{env} is low and only few people are in the lodge. The electric cycle experiences an energy shortage when a lot of people visit the lodge.

6.4.2 Modeling

Conclusions concerning the model are the following: From the results one can conclude, that the SOC of the battery E_{SOC} and the filling level of the WWTP tank $WWTP_{SOC}$ can be merged into a single state. This idea is derived in Section 6.2.3 but not implemented in this thesis. This is a very interesting result due to the fact that reducing the number of states of the model without losing information is very favorable: the optimizing algorithm is evaluated faster without loss of accuracy.
Besides that, the behavior of the heating tanks shows, that the heat transfer from the thermal solar collectors into the building takes place mainly through the daily warming up and cooling down of the LTS. This behavior is apparent in all three periods discussed in Section 6.3.
As already discussed several times in this thesis the separation of LTS and HTS leads sometimes to unrealistic behavior like in March where the CHP is turned on several times because of the LTS even though the HTS saturates immediately. Some ideas to improve the model is to change the volume ratio which splits up the two storages or even to merge the two storages into one. Either way a good model for the heating tanks depends on a not yet possible parameter identification on the real system. This concludes, that the model of the heating tanks must be proved carefully in order to derive the exact behavior of the heating system.
The link between the electric and the thermal cycle, the *electric heating*, is useful. However, from the results of the heuristic controller can be concluded, that a lack of energy in the thermal cycle cannot be compensated significantly by electric heating. Because the LTS, which shows the biggest energy shortage in the simulations, is not controllable by the electric heating. In contrast are the two other tanks, HTS and WDWS, directly respectively indirectly reachable by the electric heating.

6.4.3 Optimization

The goal to find *goa*-maximizing control inputs to a non-linear system with 6 states was achieved. The chosen way of splitting the system in a linear and a non-linear part turned out to be a success. This is first of all because either the thermal or the electric cycle has a *goa* of 100% in each time period, this fact simplifies the overall *goa* calculation a lot. This comes from the unequal booking schedule and weather impact on the two subsystems.
The implementation of the DP brought a lot of degrees of freedom, especially for the definition of the cost function, which was adapted such that reality is represented as accurate as possible. Tuning the cost assignment and the boundary conditions was an iterative procedure with the goal, that the algorithm computes realistic results.
The implementation of the LP was compared to the DP rather straight forward. Only few parameters had to be fixed (the weighting vectors q and r) which allowed a quick implementation.
The tuned algorithms compute easily interpretable results which formed the basis to gain a lot of insights into the various processes in the system.

A further benefit is some knowledge which can be gained for the tuning of HC for such systems. The most important is that on sunny days the available energy should be fed as fast as possible to the building storage instead of storing it in the LTS, which should be at a low state in the morning to save the next day's solar energy.

Bibliography

Note: All PDF files can be found on the appended CD.

[1] Bearth & Deplazes Archtitekten AG. Plan of the 1^{st} Floor of the New Monte Rosa Lodge. A4plan_OG01.pdf.

[2] Boyd S. and Vandenberghe L. *Convex Optimization*. Cambridge University Press, New York, NY, USA, 2004.

[3] Feuron. Datasheet Top Sol 1450/270. Top_Sol_1450270.pdf, 2005.

[4] Flühmann, K., Oerlikon Stationary Batteries Ltd. Phone Call about the Approximaton of the Battery. ProtokollAccuOerlikon.pdf, April 2008.

[5] Guzzella, L. Modeling and Analysis of Dynamic Systems. 2007.

[6] Guzzella, L. and Sciarretta, A. *Vehicle Propulsion Systems: Introduction to Modeling and Optimization*. Springer, Berlin ; New York, second edition, 2007. Lino Guzzella, Antonio Sciarretta. ill. ; 25 cm.

[7] Hornby, A. S. *Oxford Advanced Learner's Dictionary of Current English*. Oxford University Press, London, third edition, 1974.

[8] KW Energie Techninik. Datasheet Combined Heat and Power Plant KWE 12P4 SI. BHKW_KWE_12P4_SI.pdf, www.kwenergietechnik.de, 2008.

[9] Lauber IWISA. Design Energy Storage System. Ausfuehrung_Energiespeicher.pdf, 2008.

[10] Lauber IWISA. New Monte Rosa Lodge: Conceptual Drawing of the Heating System. Prinzipschema_Heizung.pdf, 2008.

[11] Lauber IWISA. Plan of the 1^{st} Sub Level of the New Monte Rosa Lodge. 1.UGKO.pdf, 2008.

[12] Lauber IWISA. Plan of the 2^{nd} Sub Level of the New Monte Rosa Lodge. 2.UGKO.pdf, 2008.

[13] Leibundgut, H., Baldini, L., Bollier, P., Gass, V., Meggers, F., Radaelli, E., Schlüter, A. and Thesseling, F. viaGialla. http://www.viagialla.ch, 2007.

[14] Loosli, B. New Monte Rosa Lodge: Pump Dimensioning. MonteRosa-Pumpen.pdf, 2008.

[15] Martin Systems AG, Sonneberg. Energy Balance WWTP. Energiebilanz_Rev0.pdf, 2008.

[16] Menti, U. New Monte Rosa Lodge: Energy Management and HA, Phase Documentation. Monte_Rosa_Phasendoku_061221.pdf, 2006.

[17] Menti, U. New Monte Rosa Lodge: Dimensioning of the HA. Monte_Rosa_Grundlagen_Gebaeudetechnik_060915.pdf, August 2008.

[18] Muntwyler Energietechnik AG. New Monte Rosa Lodge, Solar Energy Feed-in. Solare_Netzeinspeisung_Muntwyler.pdf, 2008.

[19] Seven Air. Datasheet Ventilation System. Datenblaetter_Seven_Air.pdf, 2008.

[20] Swiss Alpine Club SAC. Die Alpen. http://alpen.sac-cas.ch, August 2005.

[21] Tschui, A. and Plüss, I. New Monte Rosa Lodge: Energy Balance. Energiebilanz_H019_F12_Komfort.xls, September 2006.

[22] Zürcher, C. and Frank, T. *Bauphysik - Bau und Energie*, volume 2. Christoph Zürcher, 2^{nd} edition, 2004.

ETH
Eidgenössische Technische Hochschule Zürich
Swiss Federal Institute of Technology Zurich

Institut fr Mess- und Regeltechnik
Prof. L. Guzzella
Prof. R. D'Andrea

Titel der Arbeit:

Modeling of the New Monte Rosa Lodge and Determination of an Optimal Control Signal

Art der Arbeit und Datum:

Bachelorarbeit, December 2008

Betreuung:

Prof. Dr. Lino Guzzella

Studenten:

Name:	Andreas Isler
E-mail:	aisler@ethz.ch
Legi-Nr.:	05-910-047
Semester:	6

Name:	Tobias Baltensperger
E-mail:	batobias@ethz.ch
Legi-Nr.:	05-915-731
Semester:	6

Erklärung:

Wir erklären hiermit, diese Arbeit selbständig verfasst und keine anderen als die angegebenen Quellen benutzt zu haben. Alle Stellen, die wörtlich oder sinngemss aus Quellen entnommen wurden, sowie Daten und Graphiken, die aus Quellen stammen, haben wir als solche gekennzeichnet. Die Resultate sind vollstndig und wahrheitsgetreu wiedergegeben. Wir haben weder absichtlich relevante Daten weggelassen, noch Versuchs- oder Simulationsresultate manipuliert.

Zürich, 18. 12. 2008: _____